TITLE:

Salt marsh ecosystem restructuring enhances elevation resilience and carbon storage during accelerating relative sea-level rise

Short title: Salt marsh elevation resilience

AUTHORS

[1]Meagan Eagle Gonneea*
[2]Christopher V. Maio
[1]Kevin D. Kroeger
[3]Andrea Hawkes
[4]Jordan Mora
[5,7]Richard Sullivan
[5]Stephanie Madsen
[2]Richard M. Buzard
[6]Niamh Cahill
[5]Jeffrey P. Donnelly

[1]Woods Hole Coastal & Marine Science Center, U.S. Geological Survey
384 Woods Hole Rd.
Woods Hole, MA 05343
*mgonneea@usgs.gov (corresponding author), 508-457-2280
kkroeger@usgs.gov, 508-457-2270

[2] University of Alaska Fairbanks
Department of Geosciences
PO Box 755780, Fairbanks, AK 99775, USA
cvmaio@alaska.edu, 907-474-5651
rmbuzard@alaska.edu

[3]University of North Carolina Wilmington
Earth and Ocean Sciences Department
601 South College Rd., Wilmington, NC 28403, USA
hawkesa@uncw.edu

[4] Waquoit Bay National Estuarine Research Reserve
149 Waquoit Highway, Waquoit, MA 02536, USA
Jordan.mora@state.ma.us, 508-457-0495 ext. 128

[5]Woods Hole Oceanographic Institution
Coastal Systems Group
266 Woods Hole Road, Mail Stop #22, Woods Hole, MA 02543, USA

jdonnelly@whoi.edu, 1-508-289-2665
rsullivan@whoi.edu
smadsen@whoi.edu, 1-508-289-2205

[6]University College Dublin
School of Mathematics and Statistics
Belfield, Dublin 4, Ireland
niamh.cahill@ucd.ie

[7]Texas A&M University
Department of Oceanography
400 Bizzell St, College Station, TX 77843, USA
richardmsullivan@tamu.edu

Abstract:

Salt marshes respond to sea-level rise through a series of complex and dynamic bio-physical feedbacks. In this study, we found that sea-level rise triggered salt marsh habitat restructuring, with the associated vegetation changes enhancing salt marsh elevation resilience. A continuous record of marsh elevation relative to sea level that includes reconstruction of high-resolution, sub-decadal, marsh elevation over the past century, coupled with a lower-resolution 1500-year record, revealed that relative sea-level rose 1.5 ±0.4 m, following local glacial isostatic adjustment (1.2 mm/yr). As sea-level rise has rapidly accelerated, the high marsh zone dropped 11 cm within the tidal frame since 1932, leading to greater inundation and a shift to flood- and salt- tolerant low marsh species. Once the marsh platform fell to the elevation favored by low-marsh *Spartina alterniflora*, the elevation stabilized relative to sea level. Currently low marsh accretion keeps pace with sea-level rise, while present day high marsh zones that have not transitioned to low marsh have a vertical accretion deficit. Greater biomass productivity, and an expanding subsurface accommodation space favorable for salt marsh organic matter preservation, provide a positive feed-back between sea-level rise and marsh platform elevation. Carbon storage was 46 ± 28 g C/m^2/yr from 550 to 1800 CE, increasing to 129 ± 50 g C/m^2/yr in the last decade. Enhanced carbon storage is controlled by vertical accretion rates, rather than soil carbon density, and is a direct response to anthropogenic eustatic sea-level rise, ultimately providing a negative feedback on climate warming.

Highlights:

- New England salt marshes are transitioning from high to low marsh habitat under the highest rates of sea level rise in the past 1500 years.

- Low marsh transgression results in resilient marsh platform elevation due to greater low marsh productivity and organic matter accretion.

- Accelerating accretion in response to sea-level rise results in enhanced carbon storage rates in salt marshes.

Key words: salt marsh; sea-level rise; carbon storage; elevation; 14-carbon; sea level index point; accretion

Graphical abstract:

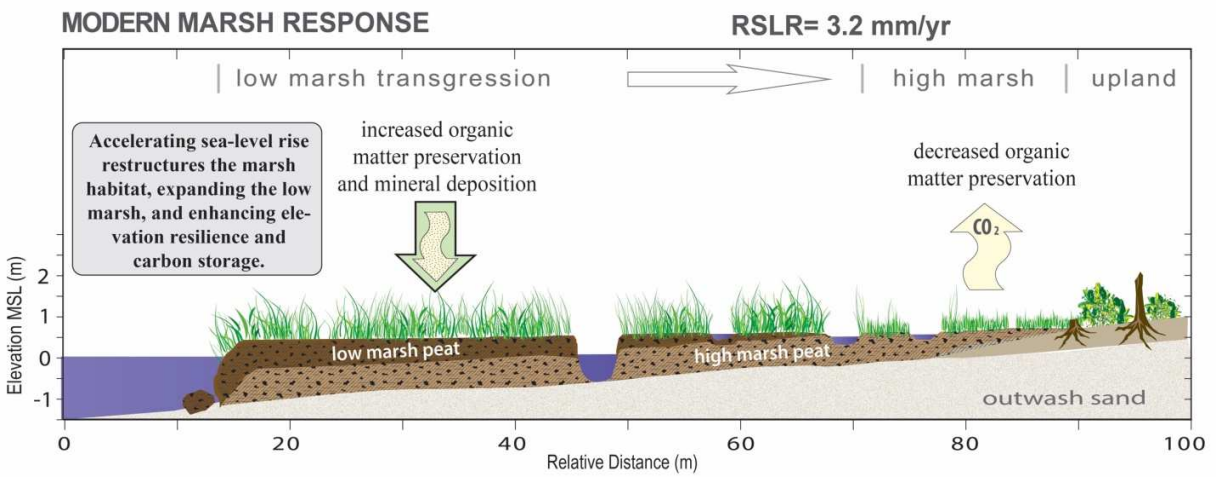

89 **1. INTRODUCTION**

90 Coastal salt marshes are vital transitional environments that provide key ecosystem
91 services, including bird, fish, and animal habitat; storm surge and erosion protection; and
92 climate benefits through long-term carbon storage (Chmura et al., 2003; Morgan et al., 2009;
93 Narayan et al., 2017; Shepard et al., 2011). Complex feedbacks between ecology—plant
94 production and decomposition—and geomorphology—sedimentation and erosion—have
95 allowed globally extant salt marshes to maintain platforms within a narrow elevation range
96 relative to sea level over thousands of years. However, they are vulnerable to coastal filling and
97 development, declining sediment supply, eutrophication, and accelerating relative sea-level rise
98 (Deegan et al., 2012; Gedan et al., 2009; Kirwan and Temmerman, 2009; Kroeger et al., 2017;
99 Weston, 2014). Given this set of challenges, there remains a great deal of uncertainty regarding
100 the capacity of salt marshes to persist in the Anthropocene under the predicted increases in the
101 rate of global eustatic sea-level rise (SLR; ~8-16 mm/yr by 2100 (IPCC, 2014)), and whether their
102 long-term ability to store carbon and provide other ecosystem services will be diminished
103 (Gedan et al., 2009).

104 While there is evidence in both experimental treatments and environmental records
105 that marsh drowning is ongoing, other marshes are transforming as salt- and flood-tolerant low
106 marsh species replace shrinking high marsh ecosystems, and still others are keeping pace with
107 relative sea level rise (Beckett et al., 2016; Crosby et al., 2016; Donnelly and Bertness, 2001;
108 Kulawardhana et al., 2015; Smith, 2015; Watson et al., 2017). Indeed, a recent review suggests
109 that marsh vulnerability has been overstated and that many marshes continue to aggrade
110 (Kirwan et al., 2016a). Both the loss of salt marsh area and the ecological shift to dominance of

111 low marsh species across the marsh platform has raised the question of whether these
112 societally important ecological systems will remain viable in the future and whether they will
113 continue to serve as important carbon stores (Chmura, 2013; Crosby et al., 2016; Holmquist et
114 al., 2018a). In an effort to answer these questions, numerous models have attempted to
115 determine marsh plant response to relative sea-level rise, as well as the associated change in
116 marsh platform accretion capacity (i.e. elevation gain) (Langley et al., 2013; Voss et al., 2013),
117 and to identify the threshold rate of relative sea-level rise under which salt marsh submergence
118 occurs (Kirwan and Mudd, 2012; Morris and Bowden, 1986; Morris et al., 2002). Vegetation
119 response to increased inundation occurs quickly, on the scale of seasons to years (Hanson et al.,
120 2016; Langley et al., 2013; Watson et al., 2015), however the implications for long-term
121 elevation resilience and carbon burial associated with this vegetation shift are not fully
122 understood, particularly at the decadal and longer time scale.
123 This study was designed to evaluate how complex ecological feedbacks between relative
124 sea level and habitat structure impact marsh elevation resilience in the face of rising sea levels.
125 Our study was conducted in four fringing salt marshes in Cape Cod, MA, USA. Marsh
126 transgression, where low marsh species move in to locations previously dominated by high
127 marsh species, has been documented in these environments (Donnelly and Bertness, 2001;
128 Smith, 2015). Prior to the recent acceleration in relative sea-level rise, these marshes kept pace
129 with relative sea-level rise rates from ~0.4 mm/yr to ~1 mm/yr (Nerem et al., 2018; Orson and
130 Howes, 1992; Redfield, 1972; Sallenger et al., 2012). Marshes such as those studied here, with
131 low tidal amplitude and minimal external sediment supply, are predicted to be among the most
132 vulnerable to sea-level rise, since accretion rates are limited to the maximum rate of organic

matter preservation (Balke et al., 2016; Kearney and Turner, 2016). Thus, these systems may serve as a symbolic "canary in the coal mine" for coastal wetland fate under a regime of accelerating rates of relative sea-level rise.

In this study we first present evidence from seven annual vegetation surveys to determine if high marsh loss is occurring through low marsh vegetation transgression. We construct sediment records of elevation change over the past 1500 years from a series of nine sea level index points (SLIPs) derived from foraminifera assemblages in AMS ^{14}C dated basal salt marsh peats, coupled with high temporal resolution ^{210}Pb age models covering the past century at four microtidal salt marshes with low sediment supply. We hypothesize that the marsh platform will lower within the tidal frame as rates of relative sea-level rise outpace marsh accretion. Greater inundation will subsequently lead to low marsh vegetation transgression into former high marsh habitat, enhancing marsh productivity and accretion rates, and providing a positive feedback to sea-level rise and thus greater elevation resilience for the entire marsh complex. We further predict that if the marsh accretion rate keeps pace with relative sea-level rise, the environment conducive to organic matter preservation will expand, enhancing carbon storage.

2. MATERIALS AND METHODS

2.1 Study area

Our study was conducted in fringing salt marshes along the southern shore of Cape Cod, Massachusetts, USA within the Waquoit Bay estuarine system (41.5°N, 70.5°W, Fig. 1). Sand and gravel outwash deposited during the melting of the Laurentide Ice Sheet, which began its retreat approximately 23,000 years ago, was subsequently reworked by fluvial, coastal, and

aeolian processes (Oldale, 1992; Uchupi et al., 1996). The reworked outwash, kettle basins, and spring sapping valleys provide the geologic framework for the back-barrier lagoon system (Gutierrez et al., 2003; Maio et al., 2014). It was not until the past 5000 years that sea-levels stabilized enough to allow for the widespread development of salt marshes on top of the reworked outwash sands of Waquoit (Orson and Howes, 1992).

Mixed semidiurnal micro-tides, with a mean range of 0.4 m (Fig. 2), protected locations within back-barrier lagoons, and the absence of large rivers, results in minimal sediment supply to these marshes. The current extent of the fringing salt marsh is discontinuous due to coastal development, which has rapidly expanded over the past 70 years. At present, the high marsh plant communities are dominated by *Spartina patens*, *Juncus gerardi* and *Distichlis spicata*, while *Spartina alterniflora* dominates the low marsh (Fig. 3) (Moseman-Valtierra et al., 2016). Salt marsh peat thickness is typically 1 to 2 m, although some sites (Hamblin Pond) have >3 m of peat (Orson and Howes, 1992). The four marshes, Sage Lot Pond (SLP), Hamblin Pond (HP), Eel Pond (EP), and Great Pond (GP), included in this study vary in size and in density of residential development on their watersheds. Thus the associated estuaries exist along a nutrient-loading gradient (0.5, 2.9, 6.3 and 12.6 g N m^{-2} y^{-1}, Valiela et al. (2000)) (Fig. 1).

2.2 Core collection and processing

Sediment cores used for radiometric dating of salt marsh accretion over the past century were collected from each of the four fringing marshes in 2013 and 2014 (3 in SLP, 3 in HP, 2 in EP and 3 in GP, Fig.1, Table S1). For the 11 cores collected for ^{210}Pb dating, the plastic core liner (diameter 11 cm) was fitted with a gasketed piston that was placed on the sediment surface. The clear, sharpened core liner was pushed down into the marsh subsurface, while

tension on the piston maintained it at the marsh surface. We visually observed the sediment surface to ensure that the soil column did not compact during collection. Once the core reached the underlying coarse sediment interface (except at HP, where the depth to the peat base was >2 m), the core liner and piston were removed from the marsh with a pulley system. Total peat recovered ranged from 14 to 150 cm using this system. The cores were split vertically, sampled at 1 cm intervals to 30 cm below soil surface and 2 cm intervals thereafter, frozen, and then freeze-dried. Dry bulk density was determined from the weight of the sediment section of known volume after freeze-drying to constant weight.

A series of 18 additional cores were collected at SLP to capture the subsurface contact between overlying high marsh peat and underlying outwash sand, representing salt marsh transgression (Fig. 1, Table 1). Cores were collected along a seaward to landward transect at nine locations approximately 3-5 m apart using a Russian peat corer to limit compaction at sites that are currently in the low marsh but were previous locations of the high marsh boundary (Fig. 1). Duplicate overlapping cores were collected to ensure preservation of the basal contact. The cores were transported to the lab in PVC casing and refrigerated at 7°C.

2.3 Short-lived radiometric dating

Approximately 5 g of dried peat was homogenized and placed on a planar-type gamma counter for 24 to 48 hours to measure ^{7}Be, ^{137}Cs, ^{210}Pb, and ^{226}Ra at 477, 661.6, 46.5 and 352 KeV energies respectively (Canberra Inc., USA). Detector efficiency was determined from the U.S. Environmental Protection Agency standard pitchblende ore in the same geometry as the samples. Activities of ^{7}Be, ^{137}Cs, and ^{210}Pb were decay corrected to time of collection.

Suppression of low energy peaks by self-absorption was corrected for (Cutshall et al., 1983). Detection limit for excess ^{210}Pb was 0.05 dpm g^{-1}. A 0.5 g aliquot of sediment was further ground in a ball mill and then analyzed for carbon (C) concentration and δ^{13}C at the U.C. Davis Stable Isotope Facility with an Elementar Vario EL Cube or Micro Cube elemental analyzer (Elementar Analysensysteme, Germany) interfaced to a PDZ Europa 20-20 isotope ratio mass spectrometer (Sercon Ltd., UK).

Sediment ages and accretion rates for the past century were calculated with the continuous rate of supply ^{210}Pb age model, a variant on the advection-decay equation (Appleby and Oldfield, 1978). This model assumes that ^{210}Pb supply to the sediment surface is constant through time, but allows for changing sedimentation rates, in addition to decay, to control the down-core activity of ^{210}Pb. Thus, this model was used to provide sufficient temporal resolution to assess decadal scale changes over the past century in these marshes. The common form of the continuous rate of supply model as derived by Appleby and Oldfield (1978) solves for age t based on the distribution of ^{210}Pb in the sediment record. Prior to application of the age model, ^{210}Pb profiles were evaluated to ensure they were sufficiently resolved to apply the continuous rate of supply model without bias towards ages that are too old or accretion rates that are too low at depth (Binford, 1990).

2.4 Radiocarbon dating

Plant macrofossils were sampled at the sandy peat transition zone between the basal sand and continuous peat, typically between 1 and 8 cm above the actual basal contact as observed in core logs. Assuming the basal peat sampled represents the establishment of the

high marsh surface at the sampled elevation, and that there is limited peat compression at the basal contact, its ^{14}C age and sampled elevation can be used as a proxy for the paleo-high marsh surface (Engelhart and Horton, 2012; Hawkes et al., 2016). Rhizomes, which grow directly below the marsh surface, belonging to the high marsh species *S. patens*, *J. gerardi* and *D. spicata,* were identified based on the key provided by Niering et al. (1977), cleaned with deionized water, and subsampled under a dissecting microscope. Seventeen samples were submitted to the National Ocean Science Accelerator Mass Spectrometry facility at the Woods Hole Oceanographic Institution for ^{14}C AMS dating. All organic-derived ^{14}C ages were calibrated using Calib version 7.0.1 with the IntCal13 calibration data set (Reimer et al., 2009) and are here reported in median calibrated years before present and median calibrated years with a 2 sigma (2σ) range of uncertainty.

2.5 Foraminifera sampling and relative sea-level reconstruction

Basal peat cores were processed for foraminiferal analysis by first identifying the basal stratigraphic contact between Pleistocene sand and overlying initial salt marsh development assumed to be high marsh peat. Iterative sampling from the contact up-core was done until foraminifera were of sufficient abundance to reasonably determine that the assemblages were *in situ*. Foraminiferal sediment samples (2 cm^3) were sieved through 500 and 63 µm sieves to isolate foraminiferal bearing sediments and avoid clays, silts, and larger organics. Dead foraminifera were counted and identified to species level using a binocular microscope. Total foraminiferal abundances in the base of basal and basal peats varied from 62 to 305 individuals with between one and three species. Only samples with sufficient foraminifera and adjacent

243 radiocarbon samples were used to produce a sea level index point in each basal core.
244 Additionally, we counted foraminifera in surrounding samples to establish that the assemblage
245 was representative of the prevailing environmental conditions at the time the sediment was
246 deposited.

247 A standard approach to the development of SLIPs was used, which allows for the
248 estimation of the elevation of former sea-level in relative time and space with associated
249 uncertainties (Engelhart and Horton, 2012). Here, we use salt marsh foraminifera as a proxy
250 sea-level indicator because of their well-established relationship with the frequency and
251 duration of tidal exposure, resulting in the elevational zoning of foraminifera assemblages from
252 the upland to the tidal flats (e.g., Edwards et al., 2004; Kemp et al., 2017). The range of tidal
253 elevation over which a particular sea-level indicator forms is called the indicative meaning,
254 which contains a midpoint termed the reference water level and an indicative range which
255 references the upper and lower elevation of the indicator (van de Plassche, 1986; Woodroffe
256 and Barlow, 2015). Relative sea level is then reconstructed by assigning a reference water level
257 and indicative range to each paleo assemblage based on their similarity to modern
258 assemblages. Ecological zonation of foraminifera assemblages are comparable across different
259 climates, marsh flora, and tidal ranges along the Atlantic coast of North America, resulting in
260 low marsh foraminifera assemblages assigned elevations between mean tide level (MTL) and
261 mean high water (MHW) and high marsh assemblages elevations between MHW and highest
262 astronomical tide (HAT) (Kemp et al., 2017).

263 To determine relative sea-level trends through time, the SLIPs presented here were
264 integrated with decadally averaged tide gauge data from Woods Hole (1932-2015) within an

Errors-In-Variables Integrated Gaussian Process (EIV-IGP) model (Cahill et al., 2015). The EIV-IGP model takes into account both the vertical (tidal frame) and temporal (radiocarbon age) uncertainties associated with individual SLIPs and also accounts for their uneven spacing through time (Hawkes et al., 2016). The EIV-IGP model uses a Gaussian process to model the evolution of the rates of sea-level change throughout the observation time period (Williams and Rasmussen, 1996). The sea-level process is derived from the rate process as the integral of the Gaussian process plus measured and estimated vertical uncertainty. Time measurement uncertainties are accounted for through setting the model in an EIV framework (Dey et al., 2000).

2.6 Vegetation sampling

The Waquoit Bay National Estuarine Research Reserve conducts yearly vegetation surveys at Sage Lot Pond (NOAA NERRS, 2017). Three transects (130 to 155 m) across the sediment core collection area were sampled every ~10 m over an elevation gradient of 90 cm from the high to low marsh (Fig. 1). Plots (1 m^2 quadrat) were permanently installed in 2011 and sampled annually in August. Vegetation distribution parameters measured include: percent cover by species to 1% if less than 15%, otherwise to 5%, with all ground cover summing to 100%, and bare sediment and wrack included in the unvegetated sediment category (overstory vegetation is not included); stem count in a 0.01 m^2 subplot; and canopy height (*S. alterniflora* only), defined as the horizontal plane of 4/5 of the plants (2011-2014) or the three individual plants closest to each of the four quadrat corners (2015-2016).

287 **2.7 Elevation control and tidal datums**

288 The marsh surface elevations at the core collection sites and vegetation plots were
289 surveyed with a Trimble Real-Time Kinematic Geographic Positioning System. All data was
290 projected to NAD 1983 Massachusetts State Plane FIPS 2001 and elevations are given relative
291 to NAVD88 with an elevation accuracy of 2-3 cm. In order to determine local tidal datums, an
292 RTK GPS-surveyed sensor collected water levels at Sage Lot Pond from January 2012 through
293 December 2016. The local tidal datum was determined by tying monthly mean datums to the
294 nearby Woods Hole station 8447930 using the modified-range ratio method for semidiurnal
295 tides (NOAA, 2003). The resulting datums are corrected to the 1983-2001 National Tidal Datum
296 Epoch, and include MSL, MHW, and the HAT that is predicted over the epoch (Fig. 2). Sage Lot
297 Pond experienced nearly the same MSL (-0.117 m NAVD88) as Woods Hole with a smaller mean
298 range of 0.442 m, MHW of 0.094 m, and HAT of 0.463 m. Water level data lapses occurred,
299 especially during winter, so only months with 95% data collection were used. To test whether
300 this seasonal sampling introduced significant bias, lapses in data collection were applied to
301 Woods Hole station measurements, resulting in higher means by 1.3 cm on average. This bias is
302 less than the estimated generalized error of these datum calculations (1.52 cm), thus the latter
303 error is considered an appropriate, conservative estimate.

304 **3. RESULTS**

305 **3.1 Modern plant community structure and elevation**

306 Six years of annual vegetation surveys reveal that across the 0.9 m elevation gradient at
307 the SLP marsh, *S. alterniflora* dominates at low elevation, -0.15 to 0.30 m relative to MSL in
308 2013 (-0.0337 m NAVD88), while at higher elevations, *D. spicata* and *J. gerardi* had a slightly

lower elevation preference (0 to 0.70 m above MSL) than *S. patens* (0 to 0.90 m above MSL, Fig. 3). The elevation distribution of each species was defined by fitting a hyperbola to the maximum vegetation cover observed at each elevation and is used only to demonstrate the preferred elevation of the high and low marsh species relative to MSL (2013 data shown in Fig. 3a). Over this time, within the high marsh elevation zone, there is a slight, but not significant, decrease in percent cover of combined high marsh species from 29 to 23% (r^2=0.64, p=0.06, Fig. 3b), while there is no significant trend in either *S. alterniflora* (r^2=0.07, p=0.61) or unvegetated sediment (r^2=0.07, p=0.62) cover. Within the high marsh elevation zone, stem density significantly declined for *S. patens* (r^2=0.87, p<0.05, Fig. 3c), with a concurrent, but not significant, increase in *J. gerardii*, (r^2=0.29, p=0.27, Fig. 3c), which has a lower elevation preference.

3.2 Bulk sediment core properties

A series of one-way ANOVA tests were conducted to evaluate differences (dry bulk density (DBD), weight % C, and C density) between the 11 cores from 4 marsh sites (cores identified A, B or C; Figs. 1, 4). Mean core DBD ranged from 0.13 to 0.17 g/cm^3; core HBC was the only one significantly lower than the other cores (p<0.05; Table S2). The Hamblin Pond cores (HBA, HBB, and HBC) had higher weight % C (mean range 27.4 to 33.9%) than all other cores (16.0 to 25.9%) except EPA (28.1%) (Table S3). Mean C density, the product of DBD and weight % C, ranged from 31.8 to 44.6 kg/m^3, with GPB having significantly lower carbon density than Hamblin Pond cores and EPB (Table S4).

330 Down-core trends were evaluated with linear regression analysis. Only four cores had
331 significant ($p<0.05$) down core trends in dry bulk density: SLPA increases (0.14 to 0.21 g/cm^3),
332 while in SLPC (0.16 to 0.13 g/cm^3), GPA (0.20 to 0.11 g/cm^3), and HBA (0.20 to 0.12 g/cm^3)
333 decreases with depth. Notably, all but four cores have significant increases in weight % C down
334 core (Table S5). However, while the trend in the high marsh transition core (SLPB) was not
335 significant ($p=0.051$), weight % C decreased steeply with depth from 30% to 7% at the base of
336 the peat (11 cm). There were only three cores with significant down-core trends in carbon
337 density, the product of DBD and weight % C: SLPA (33.2 to 66.5 kg/m^3) and HBC (36.5 to 46.8
338 kg/m^3) increase with depth, while EPB (47.6 to 35.8 kg/m^3) decreases (Table S5).
339
340 **3.3 Sediment accretion over the past century**
341 The age and accretion rate for each 1 cm section was determined with the continuous
342 rate of supply model from unsupported ^{210}Pb sediment activities and sediment density (Fig. 4)
343 (Appleby and Oldfield, 1978). The past century of deposition reaches from the surface to a
344 depth of 24 to 29 cm in the low marsh and to 11 cm at the high marsh transition site (SLPB).
345 Accretion rates are highly variable (n = 310 in 11 cores), with a range of 0.8 to 9.7 mm/yr. The
346 ten cores from the area that is now low marsh at all four sites are not statistically different from
347 each other, based on one-way ANOVA tests, so all ten cores have been merged to create a
348 unified record of accretion over the past century (Fig. 4). At these four marsh sites, there is a
349 steady rise in accretion rates since 1900. For example, in the decade from 2005-2015, mean
350 accretion rates across all low marsh sites were 4.2 ± 1.5 mm/yr, compared to 2.3 ± 1.0 mm/yr in
351 the decade from 1900-1910, with uncertainty (±) expressed as the standard deviation of all

measurements for each treatment. However, accretion rates in the Sage Lot Pond high marsh transition zone core (SLPB) were statistically disparate from low marsh rates. At this site, there were much lower accretion rates over the same two decades, 0.8 mm/yr in the first decade of the 20th century, compared to 2.1 mm/yr in the most recent decade (Fig. 4). Notably, over the past century, average accretion in the high marsh increased by 1.3 mm/yr, compared to a 1.9 ± 1.8 mm/yr increase in the low marsh. This soil core data is available in an accompanying data release through the U.S. Geological Survey ScienceBase (Gonneea et al., 2018).

3.4 Relative sea-level reconstruction and paleomarsh accretion rates

To develop a RSL curve to assess marsh response and compare paleo to modern rates of change, a total of nine sea level index points and eight terrestrial limit points spanning the last ~1500 years were developed from measured ^{14}C dates of basal peat, foraminiferal assemblages, and associated sample elevations (110 y before present (-18 cm NAVD88) to 1380 y before present (-151 cm NAVD88) (Table 1)). The SLIPs included seven base of basal peat (<5 cm above the sand contact) and two basal peat (>5cm above the sand contact) samples distributed over an elevation range of 1.24 m (Fig. 5). All foraminiferal assemblages (*Haplophragmoides* sp., *Jadammina macrescens*, and *Trochammina inflata*) represent a high marsh ecological zone (MHW to HAT), with an indicative range of ±0.18 m based on the tidal datum and modern assemblages, resulting in a total elevation uncertainty of ±0.24 m (Figs. 2 & 5A, Table 1) (Edwards et al., 2004; Kemp et al., 2015). In 8 cases, the basal peat samples were absent of foraminifera, with 4 containing thecamoebians, a fresh water testate amoeba (Kemp et al.,

2017), so these serve as terrestrial limiting points that indicate an environment above the tidal frame (>HAT).

The 9 SLIPs, 8 terrestrial limiting points, and decadally-averaged Woods Hole tide gauge data (1932-2015) were integrated within an EIV-IGP model (Cahill et al., 2015) to produce a record of RSL spanning the period between 557 and 2015 CE (Fig. 5B). There was a 1.5 ±0.4 m rise in RSL during this period (Fig. 5C). The mean rate of relative sea-level rise for the 1200-years prior to 1850 was 0.9 ±0.2 mm/yr, with the rates dipping to ~0.6 mm/yr from 1400 to 1600. Between 1850 and 2015, sea level rose at a rate of 2.3 mm/yr, with maximum rates (3.2 mm/yr) occurring in the past decade.

3.5 Carbon storage rates

Carbon storage rate refers to the amount of carbon stored per year in salt marsh sediment of various ages. Carbon storage was calculated from carbon density and vertical accretion rates and was evaluated every two centimeters over the past century based on ^{210}Pb chronology (Table S7). Carbon storage was determined at lower resolution (two to ten centimeters) to 557 CE with accretion rates and ages from the EIV-IGP model, assuming that marsh accretion was equivalent to relative sea-level rise. Carbon storage rates from 557 to 1800 CE were 39 ± 14 g C/m^2/yr, with an increase to 63 ± 18 g C/m^2/yr in the century from 1800 to 1900 (Fig. 4). Carbon storage has continued to accelerate, with rates in locations that are now low marsh reaching 76 ± 33 g C/m^2/yr from 1900-1910 and 129 ± 50 g C/m^2/yr from 2005-2015. At the same time, there has been little change in carbon storage rates at locations that are presently the high marsh transition zone (SLPB, 1900-1910: 85 ± 36 g C/m^2/yr; 2005-2015:

66 ± 11 g C/m^2/yr). There is a minimum in carbon storage in the high marsh transition zone during the 1930-40's associated with low carbon content in the sediments. However, a multiple linear regression analysis of soil carbon density, accretion rate, and carbon storage rates indicates that vertical accretion rates exert ~6.5 times greater control on carbon storage rates than does sediment carbon density (Type III Sum of Squares effect size, AR = 186, C density = 33). Thus, accretion rates exert the dominant control on carbon storage rates in these salt marshes.

4. DISCUSSION

4.1 Relative sea-level history

For the majority of the nearly 1500-year record, relative sea-level rise was relatively stable at 0.9 ±0.2 mm/yr (Fig. 5). This late Holocene stability has been documented in numerous other sea-level reconstructions (e.g., Donnelly, 2006; Kemp et al., 2017). The accretion of the paleo high marsh surface is inferred to mirror this rate and was slowly transgressing landward and upward throughout the late Holocene (Fig. 6). The collapse of the Laurentide Ice Sheet proglacial forebulge after the last glacial maximum led to coastal subsidence from Maine to Florida, with the ongoing glacial isostatic adjustment (GIA) rate varying spatially with distance from the former center of the ice sheet (Barnhardt et al., 1995; Engelhart et al., 2009; Hawkes et al., 2016). According to the predictions from the ICE-6G model (version VM5a), the current rate of coastal subsidence at our study site is 1.2 mm/yr and has been relatively constant over the past 5000 years (Peltier et al., 2015). Thus, prior to 1850, the primary driver of relative sea-level rise along the U.S. Atlantic coast was land-level changes

associated with spatially-variable GIA, as differences between these two rates (0.9 ±0.2 mm/yr and 1.2 mm/yr) are within the uncertainties of both models (Engelhart et al., 2011; Peltier et al., 2015). The recent acceleration in relative sea-level rise since 1850 can be attributed to the thermal expansion of ocean water, melting of land ice, and changes to ocean circulation patterns (Rietbroek et al., 2016; Yin et al., 2009). From 1850 to 2015, sea-level rose 2.3 mm/yr with a maximum rate (3.2 mm/yr) occurring in the last decade. These rates represent nearly a threefold increase over the previous 1500 years and provide the catalyst for ecological shifts in salt marsh structure over the past century.

4.2 Marsh transgression

Vegetation surveys conducted yearly from 2011 to 2016 at Sage Lot Pond offer some direct evidence of low marsh species transgression into former high marsh regions. A dramatic decrease in *S. patens* stem density in the high marsh zone (2825 ± 2720 to 720 ± 755 stems/m^2, r^2=0.87, $p<0.05$, Fig. 3) occurred over six years, coincident with a non-significant decrease in total high marsh species coverage (29 to 23%, r^2=0.64, p=0.06). While there was no concurrent increase in low marsh species coverage in the high marsh, such an increase has been observed over the past several decades in similar fringing marshes in Rhode Island (Donnelly and Bertness, 2001; Raposa et al., 2017) and Massachusetts (Smith, 2015). We interpret this decrease in *S. patens* stem density to be driven by increased inundation beyond this species' preferred flooding and salt tolerance regime.

Prior to 1850 the rate of high marsh vertical accretion closely mirrored the rate of relative sea-level rise, supporting lateral marsh expansion into adjacent coastal forests. Since

1932 (Woods Hole tide gauge established), the high marsh transition zone has lost 11.4 cm of elevation capital relative to sea level. Elevation capital loss rates of 1.4 mm/yr indicate that the high marsh cannot maintain lateral transgression at a sufficient pace to maintain the paleo marsh habitat structure. In addition, this is likely an underestimate of total elevation capital lost since the onset of acceleration in relative sea-level rise, as this study, and others, document the acceleration beginning as early as 1860 (Kemp et al., 2017). However, we confine this analysis to the period of instrumented sea level records. From this, we predict that the total area of high marsh habitat is declining while low marsh habitat transgresses landward, restructuring the ecological zones across the marsh platform.

The accretion response of the low marsh has been more dynamic. A segmented regression analysis of relative marsh elevation indicates that from 1932 to 1974, the area that is now low marsh also lost elevation at rates between 0.03 and 0.6 mm/yr, for a total elevation capital loss of 0.2 to 4.1 cm in 42 years. After 1974, the marsh transitioned to elevation stability and recovery relative to mean sea-level (Fig. 7). This period of elevation stability occurs when the marsh platform reaches the relative elevation where vegetation surveys indicate *S. alternaflora* dominates marsh vegetation (for this site ~17 cm above MSL, Figs. 3 & 7). For the subsequent 41 years, the marsh platform elevation relative to MSL stabilized, and in 7 of the 10 low marsh cores, regained elevation capital at relative rates of 0.06 to 1.3 mm/yr, with accretion rates of 3.4 ± 0.7 mm/yr on average, matching, and potentially slightly out-pacing, the Woods Hole instrumental relative sea-level rise rate of 3.2 mm/yr. Three low marsh cores (GPA, HPA, EPB) continued to lose elevation capital at rates of 0.2 to 0.4 mm/yr. One potential reason these cores continued to lose elevation is that they are lower in the tidal frame, so that

increased inundation results in reduced, rather than enhanced, biomass productivity, and thus are responding negatively to sea-level rise (Table S1). These portions of the marsh would potentially be identified as areas to monitor for future elevation loss.

Notably, there were no significant trends in accretion response between the four marshes, despite their twenty-fold difference in nitrogen loading rates. Thus, nitrogen loading does not appear to be a primary control on accretion rates or carbon storage in these systems, unlike field experiments that indicate a positive accretion response to nitrogen fertilization (Davis et al., 2017; Fox et al., 2012). This may be potentially due to the manner of nitrogen loading, which in these estuaries occurs mainly through atmospheric deposition and groundwater inputs to the estuary, with nitrogen likely taken up within the estuary and transformed to particulate or dissolved organic nitrogen forms prior to entering the salt marsh system through tidal exchange (Valiela et al., 2016). This is in contrast to experimental nitrogen-loading treatments that directly add inorganic nitrogen to salt marsh systems, or add nitrogen at higher rates.

Low marsh vegetation succession resulted in enhanced elevation building capacity for the marsh platform. We explore three potential mechanisms for the observed elevation recovery following vegetation succession, including 1) enhanced biomass production as low marsh species dominate the platform, 2) differential rates of organic matter preservation at the two elevation zones and at different peat depths and ages, and 3) enhanced mineral deposition. All three processes could result in elevation gains within salt marshes, which derive their volume from both organic and mineral matter.

483 **4.2.1 Role of biomass production on elevation resilience**

484 The uptick in accretion rates begins around 1974 as the marsh platform reaches the
485 elevation within the tidal frame where *S. alterniflora* dominates over high marsh species (Fig.
486 7). Biomass production in the *S. alterniflora*-dominated low marsh was 105% greater than the
487 high marsh (above ground: (low) 657 ± 133 g C/m^2, (high) 516 ± 82 g C/m^2; below ground: (low)
488 5750 g C/m^2, (high) 2605 g C/m^2 (Moseman-Valtierra et al., 2016)). If peat organic matter
489 storage is sourced solely from below ground biomass (Nyman et al., 2006), then the low marsh
490 region has a much greater capacity to not only bury carbon, but to gain elevation through
491 organic matter storage, since, in peat marshes, organic material is the main contributor to
492 elevation (Morris et al., 2016; Nyman et al., 2006). Assuming the preservation rate, or the
493 fraction of annual biomass production that is preserved in peat, is constant across marsh zones,
494 then it is possible to estimate the maximum elevation growth rate based on biomass
495 production (Morris et al., 2016). Holding preservation at 10%, based on plant lignin
496 concentration (Benner et al., 1991; Hodson et al., 1984), and using an organic matter density of
497 0.085 g/cm^3 (Morris et al., 2016), maximum vertical accretion is 6.8 mm/yr in the low marsh
498 and 3.1 mm/yr in the high marsh (i.e. 0.575 g/cm^2/yr x 0.1 g lignin/g dry weight/ 0.085 g/cm^3).
499 These theoretical values are higher than observed accretion rates based on the ^{210}Pb
500 chronology (4.2 ± 1.5 and 2.3 ± 1.0 mm/yr for the low and high marsh regions, respectively,
501 from 2005-2015). Thus, enhanced biomass production in the low marsh could potentially
502 account for the elevation gains observed during low marsh transgression as *S. alterniflora*
503 dominates marsh vegetation.

504

505 **4.2.2 Role of soil organic matter preservation on elevation resilience**

506 Since organic matter is the primary contributor to vertical accretion in marshes with
507 high weight % C (Neubauer, 2008; Turner et al., 2002), such as those in this study (16 to 42
508 weight % C), ongoing decomposition in aging peat may create apparent accretion rates that are
509 higher near the surface than at depth. As organic matter is broken down and remineralized by
510 microorganisms, carbon is lost along with the associated volume of organic matter (Neubauer,
511 2008). Thus, sediment profiles with constant organic matter inputs and ongoing decomposition
512 should exhibit a decrease in weight % C and increase in sediment density, and over time, a
513 decrease in relative marsh surface elevation. In a reconstruction of the marsh surface through
514 time, those processes would appear as an increase in accretion rate in recent deposits, as
515 observed here. We first evaluate the change in weight % C and DBD with depth to determine if
516 preservation differs between elevation zones and flooding regimes and through time. Seven of
517 the ten low marsh cores have significant increases in weight % C with depth. If conditions when
518 the peat was formed in the past are comparable to those now, this finding suggests that organic
519 matter at depth is not undergoing continual remineralization and loss in these cores. DBD,
520 which we expect to increase over time with autocompaction and remineralization (Cahoon et
521 al., 1995; Day et al., 2011), only increases significantly in one core (SLPA), while in three cores,
522 DBD significantly decreases (SLPC, GPA, HBA) (Table S5). Conversely, weight % C in the high
523 marsh transition core (SLPB) drops from 30 at the surface to 7% at depth, with only a slight
524 increase in density (0.14 to 0.17 g cm^{-3}); neither trend is significant, however, likely due in part
525 to the limited number of samples over the 14-cm peat transition profile (n=6 for weight % C,
526 n=10 for DBD).

If productivity over the entire history of the high marsh transition zone core was similar to the present day, then ongoing decomposition within the short, infrequently flooded peat profile may be responsible for the recent trend of greater accretion rates in the high marsh. Using a two-end member sediment mixing model (Morris et al., 2016), it is possible to predict soil volume losses from changes in DBD and organic matter content, with the following assumptions: 1) each fraction has a fixed density (organic matter: 0.085 g/cm^3 and mineral matter: 1.99 g/cm^3), 2) only organic matter is lost during decomposition, and 3) changes in organic matter content are due only to decomposition, not variable organic matter input and storage rates. The last assumption is unlikely to be met given the dynamic environmental conditions that have occurred over the past century in salt marshes; however, it offers a conservative approach to evaluating whether these soil records reflect real changes in accretion and carbon storage versus the signature of decomposition, since we assume all reduction in organic matter results in lost soil volume, rather than changes in organic matter reflecting environmental and depositional differences through time.

In the high marsh transition zone core (SLPB) down-core DBD increases by 21% (0.14 to 0.17 g cm^{-3}), while weight % C decreases by 77% (30 to 7%). Based on these measurements, the soil volume associated with organic matter is 65% greater at the top of the core compared to the bottom. Likewise, accretion rates are 62% greater at the surface compared to rates at depth (2.1 to 0.8 mm/yr). Thus, the entire observed accretion rate difference can be accounted for via loss of organic matter volume at depth. Moreover, it is possible that the accretion rate increase is a transient feature within the sediment column and may not yield sustained elevation gains. The environmental conditions in the high marsh transition zone, including less

549 frequent flooding and greater oxygen exposure, result in continual degradation and compaction
550 of organic matter in shallow peat.

551 For the low marsh, however, the observed accretion rate increase is interpreted as a
552 persistent feature driven by acceleration in the rate of relative sea-level rise, as discussed
553 below. In low marsh profiles, most of the significant down-core trends are opposite those
554 observed in the high marsh, with higher weight % C and lower DBD at depth. However, in the
555 soil mixing model described by Morris et al. (2016), large changes in organic content occur over
556 a narrow DBD range (0.1 to 0.2 g/cm^3), that may be difficult to resolve reliably. Thus there can
557 be a relatively large soil volume loss associated with organic matter remineralization, while dry
558 bulk density is nearly unchanged (Morris et al., 2016). We evaluate the sensitivity of the
559 modeled soil volume loss compared to the observed low marsh variability (interquartile range,
560 25-75% of all measurements) in DBD (0.03 g cm^{-3}) and weight% C (3%). The soil mixing model
561 predicts that a density change of 0.03 g cm^{-3} can result in soil volume variability of 25-50% for
562 soils with a weight % C of 25-35%, while change of 3 weight % C would be associated with a 10-
563 15% range in soil volume. The precision of the carbon analysis is much better than the DBD
564 measurement, and likely provides a more accurate assessment of the maximum potential
565 changes in organic matter content, if the entire interquartile range of observations (i.e. DBD:
566 0.03 g cm^{-3} and weight% C: 3%) has occurred in a non-detected down-core trend. A 10-15%
567 reduction in soil volume would only account for an apparent increase in accretion rates of 0.4
568 to 0.6 mm/yr, so at most 18% of the accretion rate change could be due to organic matter
569 losses that available methods cannot resolve. We conclude then that ongoing organic matter
570 loss does not account for the doubling of accretion rates in recent deposits. This observation

571 that organic matter decomposition not is driving down-core changes in %C in these low marsh
572 cores may seem counter to the previously mentioned 10% preservation of biomass production
573 used to predict marsh carbon storage (Morris et al., 2016). It may be that the expansion of an
574 environment conducive to organic matter preservation as salt marshes grow vertically in
575 response to sea-level rise effectively increases the net percent of production that preserved in
576 the subsurface.
577
578 **4.2.3 Role of mineral deposition on elevation resilience**
579 As the marsh platform lowers relative to sea level, increased flooding frequency may
580 increase sediment deposition, as sediment settles onto the marsh surface when it is inundated
581 (Kirwan and Guntenspergen, 2012; Redfield, 1972). Above ground salt marsh plant structures
582 trap sediment, thus there is likely a synergy between organic production and largely mineral
583 sediment deposition in marshes (Kolker et al., 2009). DBD can inform mineral sediment content
584 and inorganic contributions to soil volume. In the low marsh, seven cores had no significant
585 trend in sediment density, three cores do have DBD increases at the top, and one core
586 decreases at the top (Table S5). There is a weak, but significant (r^2 = 0.01, p=0.01) decrease in
587 accretion rates with increase in density. Indeed, the highest accretion rates occur at the lowest
588 sediment densities (Fig. S2). There is a weak, but significant relationship between vertical
589 accretion rates and both mineral and organic carbon mass accumulation rates (Fig. S2),
590 however the slope is approximately twice as steep for organic carbon as for mineral
591 accumulation. Organic matter accumulation likely contributes more to vertical accretion than
592 does mineral accumulation. Thus, there is evidence that as organic production increases in

593 response to higher inundation levels and shifting plant assemblages, sediment trapping by
594 plants likewise increases, but contribution to sediment volume is modest.
595 The fate of salt marshes is closely linked to elevation resilience and will likely be
596 challenged by a continued acceleration in relative sea-level rise. This study demonstrates that
597 the marsh platform has been able to build elevation after transitioning to low marsh habitat
598 through positive feedback between increased inundation and enhanced productivity. While
599 multiple models have parameterized possible relative sea-level rise thresholds for marsh
600 drowning based on relatively simple metrics, including inorganic sediment supply, tidal range,
601 and biomass productivity, it is likely potentially dynamic responses to sea-level rise, including
602 evolving ecosystem structure, are not captured in such scenarios (Kirwan and Megonigal, 2013;
603 Morris et al., 2002). Indeed, if we assume current marsh productivity rates and constant
604 preservation rates persist through the future, the maximum accretion rate possible is 6.8
605 mm/yr. This would indicate that critical ecosystem services, including carbon storage, storm
606 surge protection, habitat provision, and retention of terrestrial pollutants, may be lost under
607 predicted rates (8 to 16 mm/yr (IPCC, 2014)) of sea-level rise by 2100. However, such a
608 threshold is not responsive to future ecological dynamics. In addition, if salt marsh vertical
609 accretion rates are resilient to relative sea-level rise, as shown here and reflected in salt
610 marshes globally (Kirwan et al., 2016a), then salt marsh fate may be more closely linked to
611 migration space (Kirwan et al., 2016b) and processes that reduce marsh area, such as erosion
612 and ponding (Ganju et al., 2017; Mariotti, 2016), indicating that marsh relative sea-level rise
613 thresholds must link vertical and lateral processes.
614

615 **4.3 Carbon storage under rising sea level**

616 Higher accretion rates in recent decades have occurred as vegetation structure has
617 fundamentally changed in salt marshes. Based on the above discussion, we conclude that this
618 increase in vertical accretion rates, which enhances the elevation building capacity of salt
619 marshes, is predominantly driven by increased biomass production of the low marsh grass, *S.*
620 *alterniflora*, compared to high marsh species, *D. spicata*, *J. gerardi*, and *S. patens*, and
621 facilitated by an environment favorable to preservation, including here an expanding
622 accommodation space as sea level rises (Fig. 6). Given the minimal change in carbon density
623 with depth at these sites and across marshes nationally (Holmquist et al., 2018b), changes in
624 carbon storage are primarily driven by dynamic vertical accretion rates. This amplification of
625 carbon storage in modern sediments compared to earlier deposits had previously been
626 hypothesized to be due to ongoing organic matter degradation in older, deeper peat deposits
627 (Neubauer, 2008), but the evidence here indicates that accelerating modern accretion rates are
628 a persistent feature in salt marshes. The carbon storage capacity of low marsh environments,
629 and ultimately their survival under a regime of accelerating relative sea-level rise, depends
630 directly on the total biomass production and amount preserved in the subsurface. If the
631 present-day productivity of low marsh *S. alterniflora* is already at maximal values and
632 preservation rates are stable (here we assume the marsh can store a maximum of 10% of
633 productivity within the subsurface, a relatively unconstrained value), then the peak carbon
634 storage rate in the low marsh at these sites is 575 g C/m^2/yr. This value is double that proposed
635 by Morris et al. (2016), based on lower below ground biomass production. However, below
636 ground biomass production is variable across sites and species and is likely a function of

environmental conditions including flooding regime and salinity (Alldred et al., 2017; Tripathee and Schäfer, 2015). Thus these estimates of maximal C storage may change as further research is done considering the factors controlling production and preservation of below ground biomass.

In the high marsh transition zone, there is evidence that the apparent increase in both accretion rates and carbon storage in recent years is potentially an artifact of ongoing organic matter degradation in the older portions of the soil profile. The high marsh transition zone peat demonstrated a rapid drop in weight % C with depth consistent with higher organic matter turnover in this infrequently flooded region. We posit that long-term carbon storage rates of 46 ± 28 g C/m^2/yr, as seen prior to 1800, were at steady state with relative sea-level rise of ~1 mm/yr, and marsh platforms were likely dominated by high marsh species adapted to infrequent flooding. As relative sea-level rise accelerated, salt marshes transitioned to low marsh dominated vegetation, allowing rapid vertical expansion into an enhanced accommodation space, supporting a new, greater carbon storage rate, here observed to be 129 ± 50 g C/m^2/yr, in line with rates reported globally (Chmura et al., 2003). Enhanced carbon storage in salt marshes responding to rapid relative sea-level rise provides a negative feedback on global climate warming driven by increasing atmospheric greenhouse gas concentration, albeit a modest one, by removing atmospheric CO_2 at an enhanced rate and storing it for extended time periods in salt marsh peat. However, the potential doubling or tripling of salt marsh carbon storage under accelerating sea-level rise is likely currently offset by loss and degradation of this vulnerable habitat (Gedan et al., 2009), lessening the impact of global salt marsh response to sea-level rise on atmospheric CO_2 levels.

ACKNOWLEGEMENTS, SAMPLES and DATA

The authors would like to thank Priya Ganguli, Kara Vadman and Jennifer O'Keefe Suttles for assistance with sample collection and analysis. The authors express gratitude to Waquoit Bay National Estuarine Research Reserve, Chris Weidmen, South Cape Beach State Park, and the towns of Falmouth and Mashpee for access to field sites and collaboration at the Salt Marsh Observatory. We also thank W.R. Peltier for providing GIA data for this study. This research was done as part of Bringing Wetlands to Market, a NOAA-NERRS Collaborative and USGS-supported Project. This work was funded by the USGS LandCarbon and Coastal & Marine Geology Programs, and NSF Ocean Sciences Postdoctoral Fellowship (OCE-1323728). The National Ocean Mass Spectrometry facility at WHOI provided support for radiocarbon dating while WHOI Coastal Systems Group interns provided field and lab support. Any use of trade, firm, or product names is for descriptive purposes only and does not imply endorsement by the U.S. Government.

Data and materials availability: All core data supporting this work is available at www.ScienceBase.gov, doi:10.5066/F7H41QPP.

676 **7. REFERENCES**

677 Alldred, M., Liberti, A., Baines, S.B., 2017. Impact of salinity and nutrients on salt marsh
678 stability. Ecosphere 8, e02010. https://doi.org/10.1002/ecs2.2010
679 Appleby, P.G., Oldfield, F., 1978. The calculation of lead-210 dates assuming a constant rate of
680 supply of unsupported 210Pb to the sediment. CATENA 5, 1–8.
681 https://doi.org/10.1016/S0341-8162(78)80002-2
682 Balke, T., Stock, M., Jensen, K., Bouma, T.J., Kleyer, M., 2016. A global analysis of the seaward
683 salt marsh extent: The importance of tidal range. Water Resour. Res. 52, 3775–3786.
684 https://doi.org/10.1002/2015WR018318
685 Barnhardt, W.A., Roland Gehrels, W., Kelley, J.T., 1995. Late Quaternary relative sea-level
686 change in the western Gulf of Maine: Evidence for a migrating glacial forebulge. Geology
687 23, 317. https://doi.org/10.1130/0091-7613(1995)023<0317:LQRSLC>2.3.CO;2
688 Beckett, L.H., Baldwin, A.H., Kearney, M.S., 2016. Tidal Marshes across a Chesapeake Bay
689 subestuary are not keeping up with sea-level rise. PLOS ONE 11, e0159753.
690 https://doi.org/10.1371/journal.pone.0159753
691 Benner, R., Fogel, M.L., Sprague, E.K., 1991. Diagenesis of belowground biomass of Spartina
692 alterniflora in salt-marsh sediments. Limnol. Oceanogr. 36, 1358–1374.
693 https://doi.org/10.4319/lo.1991.36.7.1358
694 Binford, M., 1990. Calculation and uncertainty analysis of 210Pb dates for PIRLA project lake
695 sediment cores. J. Paleolimnol. 3. https://doi.org/10.1007/BF00219461
696 Cahill, N., Kemp, A.C., Horton, B.P., Parnell, A.C., 2015. Modeling sea-level change using errors-
697 in-variables integrated Gaussian processes. Ann. Appl. Stat. 9, 547–571.
698 https://doi.org/10.1214/15-AOAS824
699 Cahoon, D.R., Reed, D.J., Day, J.W., 1995. Estimating shallow subsidence in microtidal salt
700 marshes of the southeastern United States: Kaye and Barghoorn revisited. Mar. Geol.
701 128, 1–9. https://doi.org/10.1016/0025-3227(95)00087-F
702 Chmura, G.L., 2013. What do we need to assess the sustainability of the tidal salt marsh carbon
703 sink? Ocean Coast. Manag. 83, 25–31.
704 https://doi.org/10.1016/j.ocecoaman.2011.09.006
705 Chmura, G.L., Anisfeld, S.C., Cahoon, D.R., Lynch, J.C., 2003. Global carbon sequestration in
706 tidal, saline wetland soils. Glob. Biogeochem. Cycles 17.
707 https://doi.org/10.1029/2002GB001917
708 Crosby, S.C., Sax, D.F., Palmer, M.E., Booth, H.S., Deegan, L.A., Bertness, M.D., Leslie, H.M.,
709 2016. Salt marsh persistence is threatened by predicted sea-level rise. Estuar. Coast.
710 Shelf Sci. 181, 93–99. https://doi.org/10.1016/j.ecss.2016.08.018
711 Cutshall, N.H., Larsen, I.L., Olsen, C.R., 1983. Direct analysis of 210Pb in sediment samples: Self-
712 absorption corrections. Nucl. Instrum. Methods Phys. Res. 206, 309–312.
713 https://doi.org/10.1016/0167-5087(83)91273-5
714 Davis, J., Currin, C., Morris, J.T., 2017. Impacts of fertilization and tidal inundation on elevation
715 change in microtidal, low relief salt marshes. Estuaries Coasts 40, 1677–1687.
716 https://doi.org/10.1007/s12237-017-0251-0
717 Day, J.W., Kemp, G.P., Reed, D.J., Cahoon, D.R., Boumans, R.M., Suhayda, J.M., Gambrell, R.,
718 2011. Vegetation death and rapid loss of surface elevation in two contrasting Mississippi

719 delta salt marshes: The role of sedimentation, autocompaction and sea-level rise. Ecol.
720 Eng. 37, 229–240. https://doi.org/10.1016/j.ecoleng.2010.11.021
721 Deegan, L.A., Johnson, D.S., Warren, R.S., Peterson, B.J., Fleeger, J.W., Fagherazzi, S., Wollheim,
722 W.M., 2012. Coastal eutrophication as a driver of salt marsh loss. Nature 490, 388–392.
723 https://doi.org/10.1038/nature11533
724 Dey, D., Ghosh, S.K., Mallick, B.K. (Eds.), 2000. Generalized linear models: a Bayesian
725 perspective, Biostatistics. Marcel Dekker, New York.
726 Donnelly, J.P., 2006. A revised late Holocene sea-Level lecord for northern Massachusetts, USA.
727 J. Coast. Res. 225, 1051–1061. https://doi.org/10.2112/04-0207.1
728 Donnelly, J.P., Bertness, M.D., 2001. Rapid shoreward encroachment of salt marsh cordgrass in
729 response to accelerated sea-level rise. Proc. Natl. Acad. Sci. 98, 14218–14223.
730 https://doi.org/10.1073/pnas.251209298
731 Edwards, R.J., Wright, A.J., van de Plassche, O., 2004. Surface distributions of salt-marsh
732 foraminifera from Connecticut, USA: Modern analogues for high-resolution sea level
733 studies. Mar. Micropaleontol. 51, 1–21.
734 https://doi.org/10.1016/j.marmicro.2003.08.002
735 Engelhart, S.E., Horton, B.P., 2012. Holocene sea level database for the Atlantic coast of the
736 United States. Quat. Sci. Rev. 54, 12–25.
737 https://doi.org/10.1016/j.quascirev.2011.09.013
738 Engelhart, S.E., Horton, B.P., Douglas, B.C., Peltier, W.R., Tornqvist, T.E., 2009. Spatial variability
739 of late Holocene and 20th century sea-level rise along the Atlantic coast of the United
740 States. Geology 37, 1115–1118. https://doi.org/10.1130/G30360A.1
741 Engelhart, S.E., Peltier, W.R., Horton, B.P., 2011. Holocene relative sea-level changes and glacial
742 isostatic adjustment of the U.S. Atlantic coast. Geology 39, 751–754.
743 https://doi.org/10.1130/G31857.1
744 Fox, L., Valiela, I., Kinney, E.L., 2012. Vegetation cover and elevation in long-term experimental
745 nutrient-enrichment plots in Great Sippewissett Salt Marsh, Cape Cod, Massachusetts:
746 Implications fore and sea level rise. Estuaries Coasts 35, 445–458.
747 https://doi.org/10.1007/s12237-012-9479-x
748 Ganju, N.K., Defne, Z., Kirwan, M.L., Fagherazzi, S., D'Alpaos, A., Carniello, L., 2017. Spatially
749 integrative metrics reveal hidden vulnerability of microtidal salt marshes. Nat. Commun.
750 8, 14156. https://doi.org/10.1038/ncomms14156
751 Gedan, K.B., Silliman, B.R., Bertness, M.D., 2009. Centuries of human-driven change in salt
752 marsh ecosystems. Annu. Rev. Mar. Sci. 1, 117–141.
753 https://doi.org/10.1146/annurev.marine.010908.163930
754 Gonneea, M., Kroeger, K., O'Keefe-Suttles, J., 2018. Collection, analysis, and age-dating of
755 sediment cores from salt marshes on the south shore of Cape Cod, Massachusetts, from
756 2013 through 2014. https://doi.org/10.5066/F7H41QPP
757 Gutierrez, B.., Uchupi, E., Driscoll, N., Aubrey, D., 2003. Relative sea-level rise and the
758 development of valley-fill and shallow-water sequences in Nantucket Sound,
759 Massachusetts. Mar. Geol. 193, 295–314. https://doi.org/10.1016/S0025-
760 3227(02)00665-5
761 Hanson, A., Johnson, R., Wigand, C., Oczkowski, A., Davey, E., Markham, E., 2016. Responses of
762 *Spartina alterniflora* to multiple stressors: Changing precipitation patterns, accelerated

763 sea level rise, and nutrient enrichment. Estuaries Coasts 39, 1376–1385.
764 https://doi.org/10.1007/s12237-016-0090-4
765 Hawkes, A.D., Kemp, A.C., Donnelly, J.P., Horton, B.P., Peltier, W.R., Cahill, N., Hill, D.F., Ashe, E.,
766 Alexander, C.R., 2016. Relative sea-level change in northeastern Florida (USA) during the
767 last ~8.0 ka. Quat. Sci. Rev. 142, 90–101.
768 https://doi.org/10.1016/j.quascirev.2016.04.016
769 Hodson, R.E., Christian, R.R., Maccubbin, A.E., 1984. Lignocellulose and lignin in the salt marsh
770 grass Spartina alterniflora: initial concentrations and short-term, post-depositional
771 changes in detrital matter. Mar. Biol. 81, 1–7. https://doi.org/10.1007/BF00397619
772 Holmquist, J., Windham-Myers, L., Bernal, B., Byrd, K.B., Crooks, S., Gonneea, M.E., Herold, N.,
773 Knox, S.H., Kroeger, K., McCombs, J., Megonigal, J.P., Meng, L., Morris, J.T., Sutton-Grier,
774 A.E., Troxler, T.G., Weller, D., 2018. Uncertainty in United States coastal wetland
775 greenhouse gas inventorying. Environ. Res. Lett. https://doi.org/10.1088/1748-
776 9326/aae157
777 Holmquist, J.R., Windham-Myers, L., Bliss, N., Crooks, S., Morris, J.T., Megonigal, J.P., Troxler, T.,
778 Weller, D., Callaway, J., Drexler, J., Ferner, M.C., Gonneea, M.E., Kroeger, K.D., Schile-
779 Beers, L., Woo, I., Buffington, K., Breithaupt, J., Boyd, B.M., Brown, L.N., Dix, N., Hice, L.,
780 Horton, B.P., MacDonald, G.M., Moyer, R.P., Reay, W., Shaw, T., Smith, E., Smoak, J.M.,
781 Sommerfield, C., Thorne, K., Velinsky, D., Watson, E., Grimes, K.W., Woodrey, M., 2018.
782 Accuracy and precision of tidal wetland soil carbon mapping in the conterminous United
783 States. Sci. Rep. 8. https://doi.org/10.1038/s41598-018-26948-7
784 IPCC, 2014. Climate Change 2014: Synthesis report. Intergovernmental Panel on Climate
785 Change, Geneva, Switzerland.
786 Kearney, M.S., Turner, R.E., 2016. Microtidal marshes: Can these widespread and fragile
787 marshes survive increasing climate–sea level variability and human action? J. Coast. Res.
788 319, 686–699. https://doi.org/10.2112/JCOASTRES-D-15-00069.1
789 Kemp, A.C., Dutton, A., Raymo, M.E., 2015. Paleo constraints on future sea-level rise. Curr. Clim.
790 Change Rep. 1, 205–215. https://doi.org/10.1007/s40641-015-0014-6
791 Kemp, A.C., Hill, T.D., Vane, C.H., Cahill, N., Orton, P.M., Talke, S.A., Parnell, A.C., Sanborn, K.,
792 Hartig, E.K., 2017. Relative sea-level trends in New York City during the past 1500 years.
793 The Holocene 27, 1169–1186. https://doi.org/10.1177/0959683616683263
794 Kirwan, M., Temmerman, S., 2009. Coastal marsh response to historical and future sea-level
795 acceleration. Quat. Sci. Rev. 28, 1801–1808.
796 https://doi.org/10.1016/j.quascirev.2009.02.022
797 Kirwan, M.L., Guntenspergen, G.R., 2012. Feedbacks between inundation, root production, and
798 shoot growth in a rapidly submerging brackish marsh: Marsh root growth under sea
799 level rise. J. Ecol. 100, 764–770. https://doi.org/10.1111/j.1365-2745.2012.01957.x
800 Kirwan, M.L., Mudd, S.M., 2012. Response of salt-marsh carbon accumulation to climate
801 change. Nature 489, 550–553. https://doi.org/10.1038/nature11440
802 Kirwan, M.L., Megonigal, J.P., 2013. Tidal wetland stability in the face of human impacts and
803 sea-level rise. Nature 504, 53–60. https://doi.org/10.1038/nature12856
804 Kirwan, M.L., Temmerman, S., Skeehan, E.E., Guntenspergen, G.R., Fagherazzi, S., 2016a.
805 Overestimation of marsh vulnerability to sea level rise. Nat. Clim. Change 6, 253–260.
806 https://doi.org/10.1038/nclimate2909

807 Kirwan, M.L., Walters, D.C., Reay, W.G., Carr, J.A., 2016b. Sea level driven marsh expansion in a
808 coupled model of marsh erosion and migration. Geophys. Res. Lett. 43, 4366–4373.
809 https://doi.org/10.1002/2016GL068507
810 Kolker, A.S., Goodbred, S.L., Hameed, S., Cochran, J.K., 2009. High-resolution records of the
811 response of coastal wetland systems to long-term and short-term sea-level variability.
812 Estuar. Coast. Shelf Sci. 84, 493–508. https://doi.org/10.1016/j.ecss.2009.06.030
813 Kroeger, K.D., Crooks, S., Moseman-Valtierra, S., Tang, J., 2017. Restoring tides to reduce
814 methane emissions in impounded wetlands: A new and potent Blue Carbon climate
815 change intervention. Sci. Rep. 7. https://doi.org/10.1038/s41598-017-12138-4
816 Kulawardhana, R.W., Feagin, R.A., Popescu, S.C., Boutton, T.W., Yeager, K.M., Bianchi, T.S.,
817 2015. The role of elevation, relative sea-level history and vegetation transition in
818 determining carbon distribution in Spartina alterniflora dominated salt marshes. Estuar.
819 Coast. Shelf Sci. 154, 48–57. https://doi.org/10.1016/j.ecss.2014.12.032
820 Langley, A.J., Mozdzer, T.J., Shepard, K.A., Hagerty, S.B., Patrick Megonigal, J., 2013. Tidal marsh
821 plant responses to elevated CO2 , nitrogen fertilization, and sea level rise. Glob. Change
822 Biol. 19, 1495–1503. https://doi.org/10.1111/gcb.12147
823 Maio, C.V., Gontz, A.M., Weidman, C.R., Donnelly, J.P., 2014. Late Holocene marine
824 transgression and the drowning of a coastal forest: Lessons from the past, Cape Cod,
825 Massachusetts, USA. Palaeogeogr. Palaeoclimatol. Palaeoecol. 393, 146–158.
826 https://doi.org/10.1016/j.palaeo.2013.11.018
827 Mariotti, G., 2016. Revisiting salt marsh resilience to sea level rise: Are ponds responsible for
828 permanent land loss? J. Geophys. Res. Earth Surf. 121, 1391–1407.
829 https://doi.org/10.1002/2016JF003900
830 Morgan, P.A., Burdick, D.M., Short, F.T., 2009. The functions and values of fringing salt marshes
831 in northern New England, USA. Estuaries Coasts 32, 483–495.
832 https://doi.org/10.1007/s12237-009-9145-0
833 Morris, J.T., Barber, D.C., Callaway, J.C., Chambers, R., Hagen, S.C., Hopkinson, C.S., Johnson,
834 B.J., Megonigal, P., Neubauer, S.C., Troxler, T., Wigand, C., 2016. Contributions of
835 organic and inorganic matter to sediment volume and accretion in tidal wetlands at
836 steady state: Sediment bulk density and ignition loss. Earths Future 4, 110–121.
837 https://doi.org/10.1002/2015EF000334
838 Morris, J.T., Bowden, W.B., 1986. A Mechanistic, Numerical Model of Sedimentation,
839 Mineralization, and Decomposition for Marsh Sediments1. Soil Sci. Soc. Am. J. 50, 96.
840 https://doi.org/10.2136/sssaj1986.03615995005000010019x
841 Morris, J.T., Sundareshwar, P.V., Nietch, C.T., Kjerfve, B., Cahoon, D.R., 2002. Responses of
842 coastal wetlands to rising sea level. Ecology 83, 2869–2877.
843 https://doi.org/10.1890/0012-9658(2002)083[2869:ROCWTR]2.0.CO;2
844 Moseman-Valtierra, S., Abdul-Aziz, O.I., Tang, J., Ishtiaq, K.S., Morkeski, K., Mora, J., Quinn, R.K.,
845 Martin, R.M., Egan, K., Brannon, E.Q., Carey, J., Kroeger, K.D., 2016. Carbon dioxide
846 fluxes reflect plant zonation and belowground biomass in a coastal marsh. Ecosphere 7,
847 e01560. https://doi.org/10.1002/ecs2.1560
848 Narayan, S., Beck, M.W., Wilson, P., Thomas, C.J., Guerrero, A., Shepard, C.C., Reguero, B.G.,
849 Franco, G., Ingram, J.C., Trespalacios, D., 2017. The value of coastal wetlands for flood

damage reduction in the Northeastern USA. Sci. Rep. 7. https://doi.org/10.1038/s41598-017-09269-z
Nerem, R.S., Beckley, B.D., Fasullo, J.T., Hamlington, B.D., Masters, D., Mitchum, G.T., 2018. Climate-change–driven accelerated sea-level rise detected in the altimeter era. Proc. Natl. Acad. Sci. 115, 2022–2025. https://doi.org/10.1073/pnas.1717312115
Neubauer, S.C., 2008. Contributions of mineral and organic components to tidal freshwater marsh accretion. Estuar. Coast. Shelf Sci. 78, 78–88. https://doi.org/10.1016/j.ecss.2007.11.011
Niering, W.A., Warren, R.S., Weymouth, C.G., 1977. Our dynamic tidal marshes: Vegetation changes as revealed by peat analysis. Conn. Arbor. Bull. 22, 12.
NOAA, 2003. Computational Techniques for Tidal Datums Handbook, NOAA special publication; NOS CO-OPS 2. General Books LLC.
NOAA National Estuarine Research Reserve System (NERRS), 2017. System-wide Monitoring Program. Data accessed from the NOAA NERRS Centralized Data Management Office website: http://www.nerrsdata.org/.
Nyman, J.A., Walters, R.J., Delaune, R.D., Patrick, W.H., 2006. Marsh vertical accretion via vegetative growth. Estuar. Coast. Shelf Sci. 69, 370–380. https://doi.org/10.1016/j.ecss.2006.05.041
Oldale, R.N., 1992. Cape Cod and the Islands: The geologic story. Parnassus Imprints.
Orson, R.A., Howes, B.L., 1992. Salt marsh development studies at Waquoit Bay, Massachusetts: Influence of geomorphology on long-term plant community structure. Estuar. Coast. Shelf Sci. 35, 453–471. https://doi.org/10.1016/S0272-7714(05)80025-3
Peltier, W.R., Argus, D.F., Drummond, R., 2015. Space geodesy constrains ice age terminal deglaciation: The global ICE-6G_C (VM5a) model: Global glacial isostatic adjustment. J. Geophys. Res. Solid Earth 120, 450–487. https://doi.org/10.1002/2014JB011176
Raposa, K.B., Weber, R.L.J., Ekberg, M.C., Ferguson, W., 2017. Vegetation dynamics in Rhode Island salt marshes during a period of accelerating sea level rise and extreme sea level events. Estuaries Coasts 40, 640–650. https://doi.org/10.1007/s12237-015-0018-4
Redfield, A.C., 1972. Development of a New England salt marsh. Ecol. Monogr. 42, 201–237. https://doi.org/10.2307/1942263
Reimer, P.J., Baillie, M.G.L., Bard, E., Bayliss, A., Beck, J.W., Blackwell, P.G., Bronk Ramsey, C., Buck, C.E., Burr, G.S., Edwards, R.L., Friedrich, M., Grootes, P.M., Guilderson, T.P., Hajdas, I., Heaton, T.J., Hogg, A.G., Hughen, K.A., Kaiser, K.F., Kromer, B., McCormac, F.G., Manning, S.W., Reimer, R.W., Richards, D.A., Southon, J.R., Talamo, S., Turney, C.S.M., van der Plicht, J., Weyhenmeyer, C.E., 2009. IntCal09 and Marine09 radiocarbon age calibration curves, 0–50,000 years cal BP. Radiocarbon 51, 1111–1150. https://doi.org/10.1017/S0033822200034202
Rietbroek, R., Brunnabend, S.-E., Kusche, J., Schröter, J., Dahle, C., 2016. Revisiting the contemporary sea-level budget on global and regional scales. Proc. Natl. Acad. Sci. 113, 1504–1509. https://doi.org/10.1073/pnas.1519132113
Sallenger, A.H., Doran, K.S., Howd, P.A., 2012. Hotspot of accelerated sea-level rise on the Atlantic coast of North America. Nat. Clim. Change 2, 884–888. https://doi.org/10.1038/nclimate1597

893 Shepard, C.C., Crain, C.M., Beck, M.W., 2011. The protective role of coastal marshes: A
894 systematic review and meta-analysis. PLoS ONE 6, e27374.
895 https://doi.org/10.1371/journal.pone.0027374
896 Smith, S.M., 2015. Vegetation change in salt marshes of Cape Cod National Seashore
897 (Massachusetts, USA) between 1984 and 2013. Wetlands 35, 127–136.
898 https://doi.org/10.1007/s13157-014-0601-7
899 Tripathee, R., Schäfer, K.V.R., 2015. Above- and belowground biomass allocation in four
900 dominant salt marsh species of the Eastern United States. Wetlands 35, 21–30.
901 https://doi.org/10.1007/s13157-014-0589-z
902 Turner, R.E., Swenson, E.M., Milan, C.S., 2002. Organic and inorganic contributions to vertical
903 accretion in salt marsh sediments, in: Weinstein, M.P., Kreeger, D.A. (Eds.), Concepts
904 and Controversies in Tidal Marsh Ecology. Kluwer Academic Publishers, Dordrecht, pp.
905 583–595. https://doi.org/10.1007/0-306-47534-0_27
906 Uchupi, E., Giese, G.S., Aubrey, D.G., Kim, D.J., 1996. The Late Quaternary construction of Cape
907 Cod, Massachusetts: A reconsideration of the W. M. Davis model, in: Special Paper 309:
908 The Late Quaternary Construction of Cape Cod, Massachusetts: A Reconsideration of the
909 W. M. Davis Model. Geological Society of America, pp. 1–69. https://doi.org/10.1130/0-
910 8137-2309-4.1
911 Valiela, I., Geist, M., McClelland, J., Tomasky, G., 2000. Nitrogen loading from watersheds to
912 estuaries: Verification of the Waquoit Bay Nitrogen Loading Model. Biogeochemistry 49,
913 277–293. https://doi.org/10.1023/A:1006345024374
914 Valiela, I., Owens, C., Elmstrom, E., Lloret, J., 2016. Eutrophication of Cape Cod estuaries: Effect
915 of decadal changes in global-driven atmospheric and local-scale wastewater nutrient
916 loads. Mar. Pollut. Bull. 110, 309–315. https://doi.org/10.1016/j.marpolbul.2016.06.047
917 Voss, C.M., Christian, R.R., Morris, J.T., 2013. Marsh macrophyte responses to inundation
918 anticipate impacts of sea-level rise and indicate ongoing drowning of North Carolina
919 marshes. Mar. Biol. 160, 181–194. https://doi.org/10.1007/s00227-012-2076-5
920 van de Plassche, O. (Ed.), 1986. Sea-Level Research. Springer Netherlands, Dordrecht.
921 https://doi.org/10.1007/978-94-009-4215-8
922 Watson, E.B., Andrews, H.M., Fischer, A., Cencer, M., Coiro, L., Kelley, S., Wigand, C., 2015.
923 Growth and photosynthesis responses of two co-occurring marsh grasses to inundation
924 and varied nutrients. Botany 93, 671–683. https://doi.org/10.1139/cjb-2015-0055
925 Watson, E.B., Wigand, C., Davey, E.W., Andrews, H.M., Bishop, J., Raposa, K.B., 2017. Wetland
926 loss patterns and inundation-productivity relationships prognosticate widespread salt
927 marsh loss for Southern New England. Estuaries Coasts 40, 662–681.
928 https://doi.org/10.1007/s12237-016-0069-1
929 Weston, N.B., 2014. Declining sediments and rising Seas: An unfortunate convergence for tidal
930 wetlands. Estuaries Coasts 37, 1–23. https://doi.org/10.1007/s12237-013-9654-8
931 Williams, C.K.I., Rasmussen, C.E., 1996. Gaussian processes for regression, in: Advances in
932 Neural Information Processing Systems 8. MIT.
933 Woodroffe, S.A., Barlow, N.L.M., 2015. Reference water level and tidal datum, in: Shennan, I.,
934 Long, A.J., Horton, B.P. (Eds.), Handbook of Sea-Level Research. John Wiley & Sons, Ltd,
935 Chichester, UK, pp. 171–180. https://doi.org/10.1002/9781118452547.ch11

936 Yin, J., Schlesinger, M.E., Stouffer, R.J., 2009. Model projections of rapid sea-level rise on the
937 northeast coast of the United States. Nat. Geosci. 2, 262–266.
938 https://doi.org/10.1038/ngeo462
939

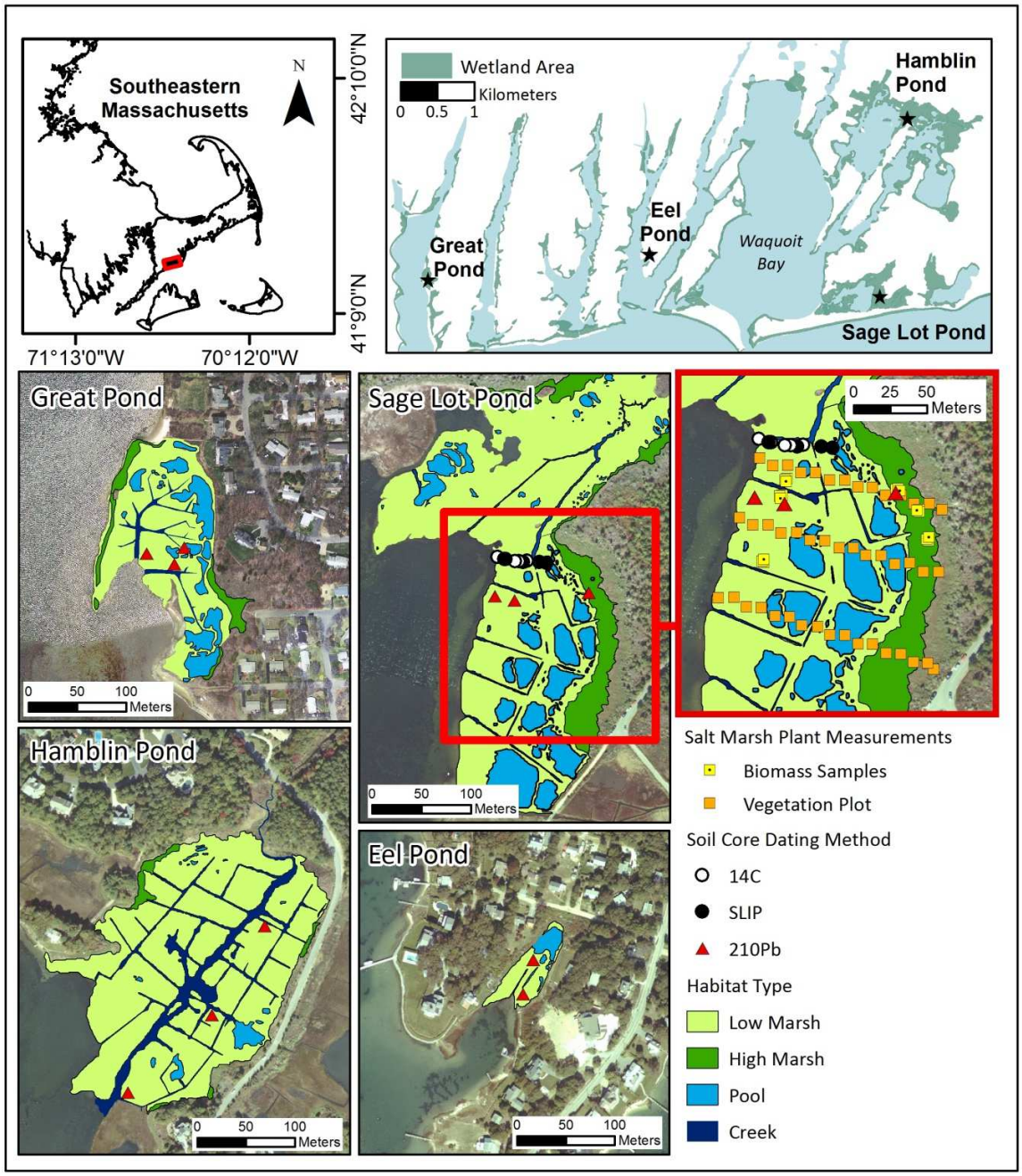

Figure 1: Location map, vegetation zones, and location of field sampling for the four salt marshes in this study. The top right panel indicates the extent of salt marsh ecosystems in the area. High marsh species include *S. patens*, *J. gerardi* and *D. spicata*, while *S. alterniflora* dominates the low marsh. Squares indicate where biomass and vegetation sampling occurred in Sage Lot Pond. Triangles indicate where cores collected for ^{210}Pb age models were collected in all four marshes. Circles indicate locations of basal peat collection for ^{14}C age dating.

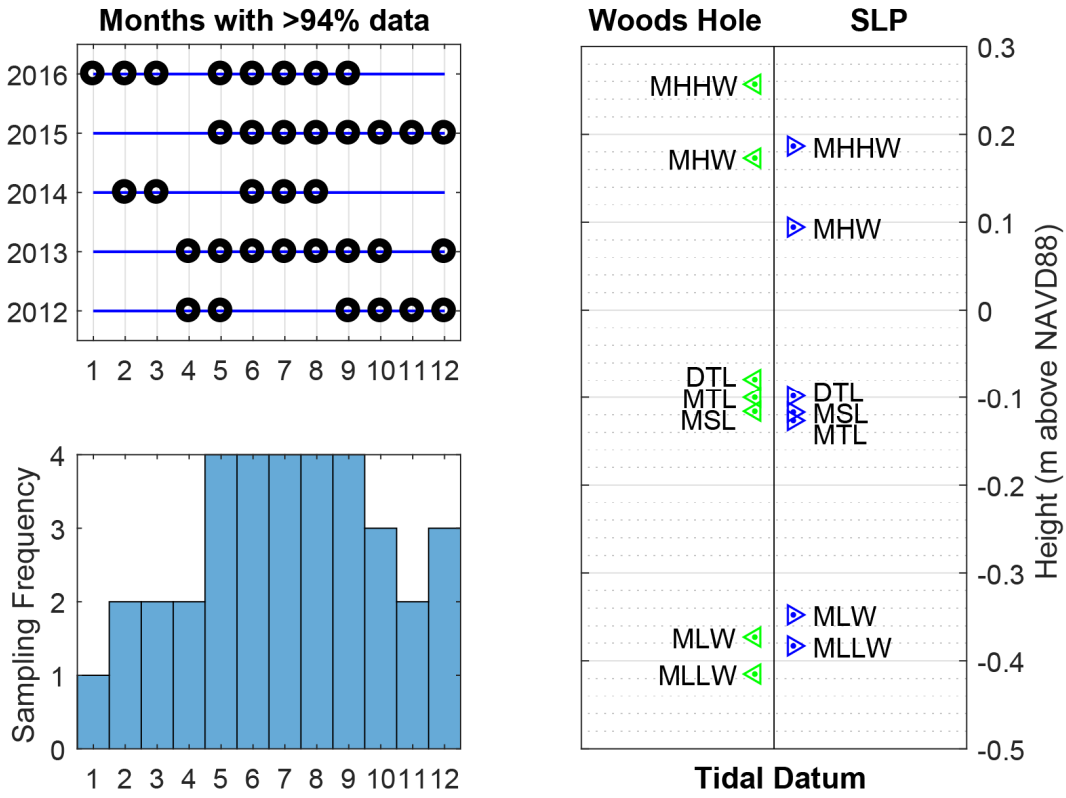

Figure 2. (Right) Tidal datums corrected for Sage Lot Pond (SLP, blue) based on nearby Woods Hole NOAA station 8447930 (green) for the 1983-2001 National Tidal Datum Epoch. (Left) Monthly means are used when calculating tidal datums, but lapses in data collection led to gaps in sampling. Only months with 95% data collection were used, and each month was sampled at least once over the six-year period.

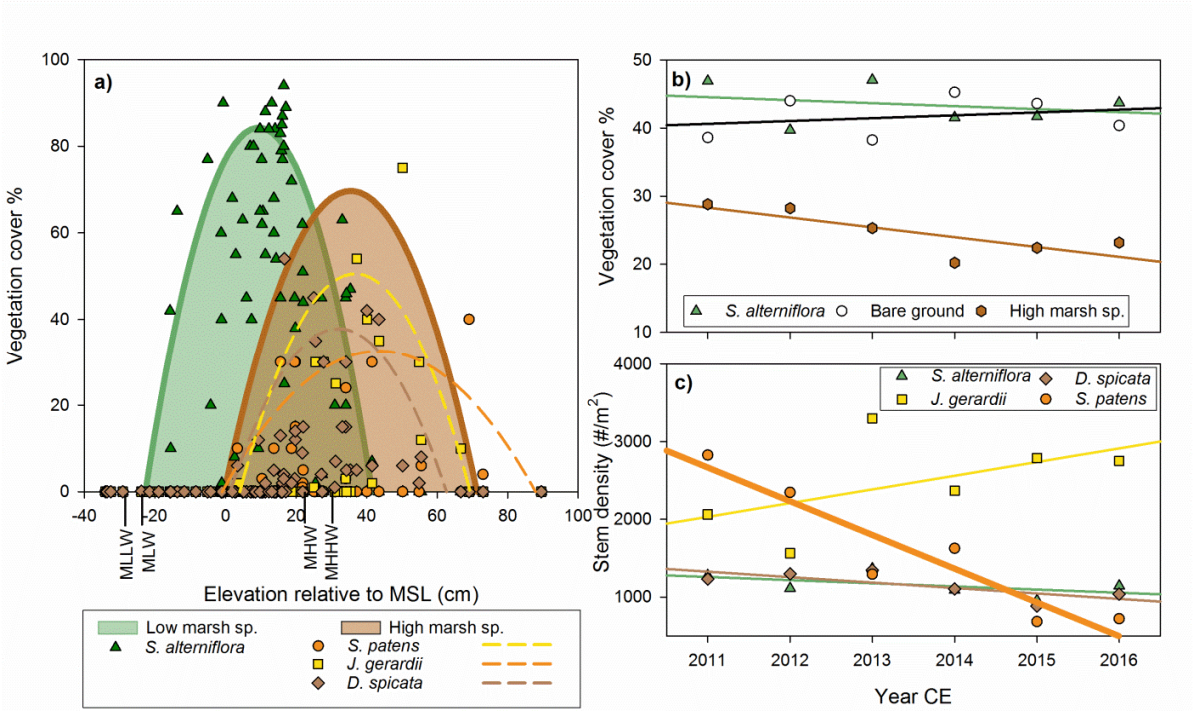

Figure 3: a) Species cover in 2013 at Sage Lot Pond across marsh elevation relative to mean sea level (MSL) in 2013. Species distributions models are shown in shaded hyperbolas as a function of elevation. b) Vegetation cover trends from 2011 to 2016. All high marsh species, *S. patens*, *J. gerardi* and *D. spicata*, are summed together and show a decreasing, but insignificant trend. c) Stem density by species indicates that *S. patens* has undergone a significant (thick line, r^2=0.87, p<0.05) reduction over the 6 years. *J. gerardi* density has increased, but not significantly (r^2=0.29, p=0.27).

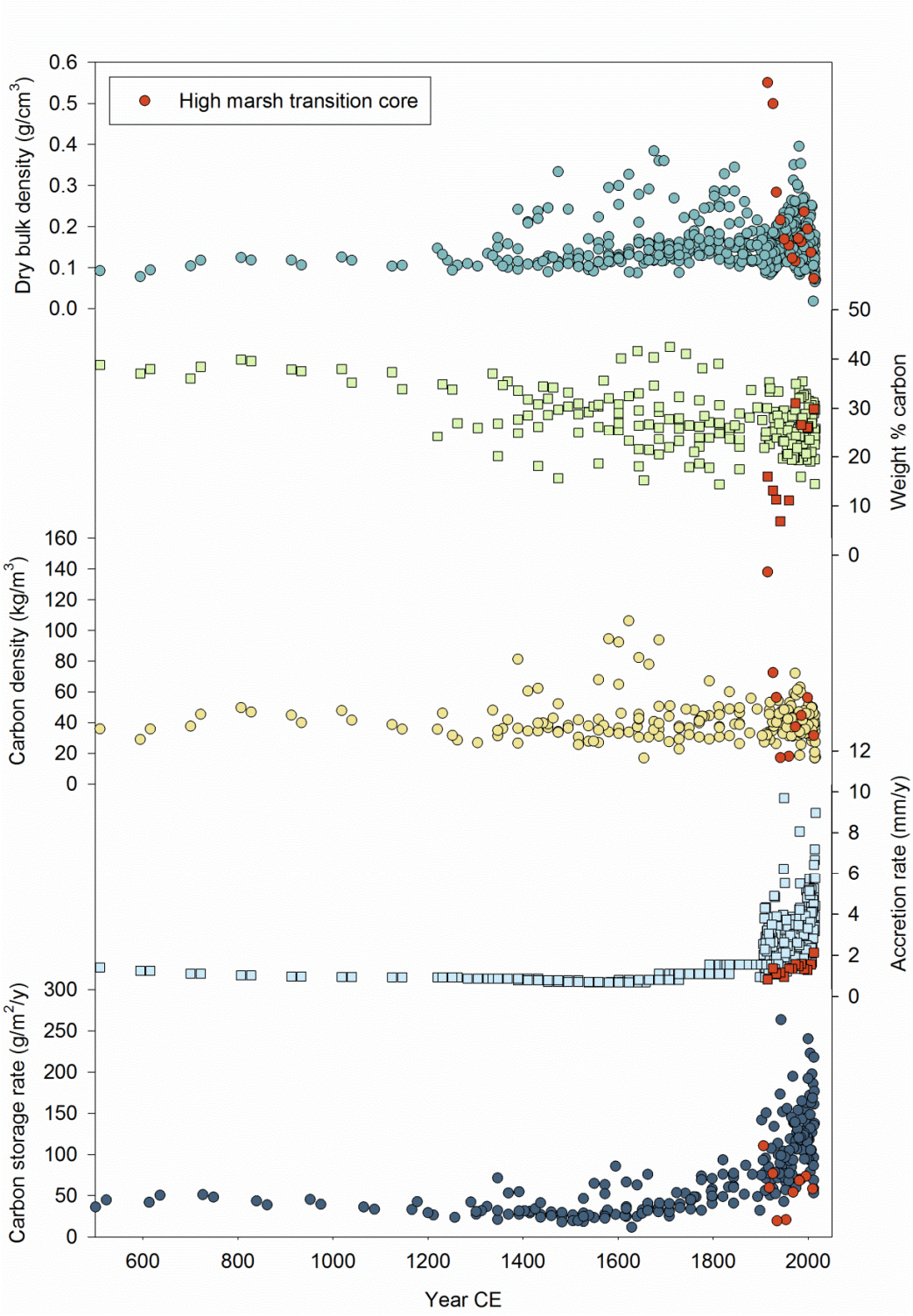

Figure 4: Dry bulk density, weight % C, C density, accretion rate, and carbon storage through time. In all plots, red symbols are the high marsh transition zone core (SLPB). Accretion rates prior to 1900 are based on EIV-IGP modeling of SLIP ^{14}C dates and elevations.

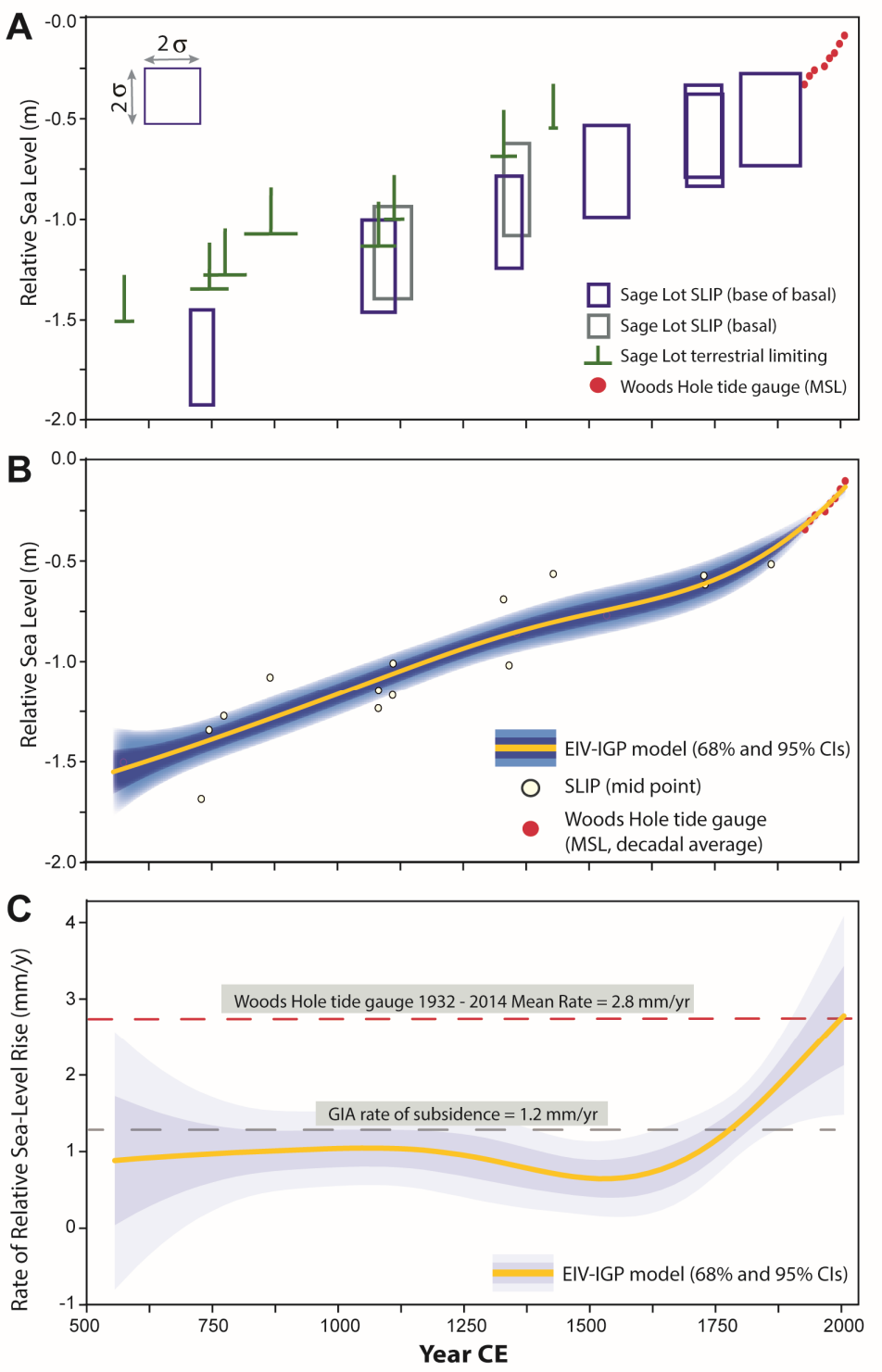

Figure 5. Relative sea-level reconstruction for Sage Lot Pond marsh. A) 9 Sage Lot SLIPs and 8 Sage Lot limiting points shown with 2 sigma vertical and temporal uncertainty window (rectangles). Key to data type in lower right. B) Modeled relative sea level record (yellow) relative to NAVD88 shown with 68% (light blue) and 95% (dark blue) confidence intervals.

Midpoints of SLIPs and limiting data shown with tan circles. Data key is shown at bottom. C) Median probability rate of relative sea-level rise (yellow line) shown with 68% (light gray) and 95% (dark gray) confidence intervals. Red dashed line shows rate of rise recorded at Woods Hole tide gauge since 1932. Gray dashed line marks the background GIA.

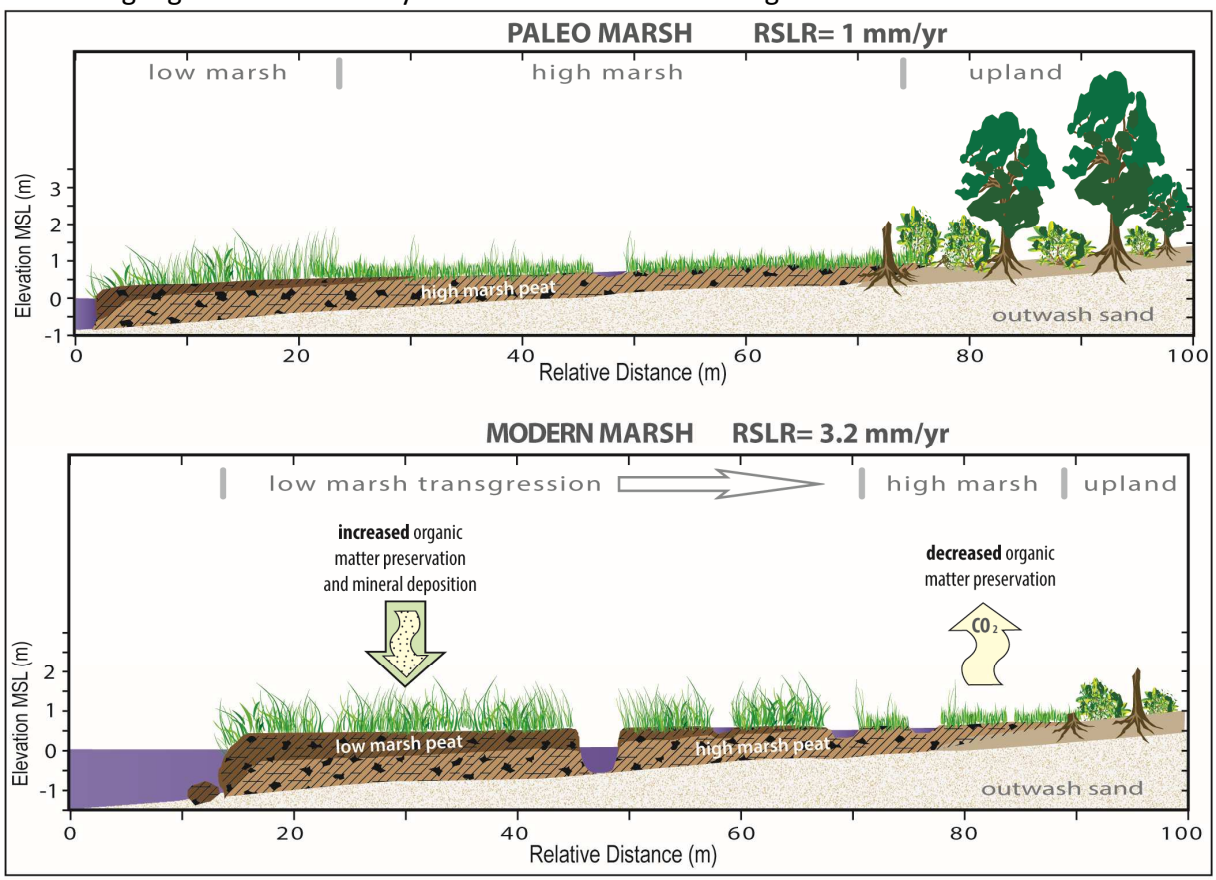

Figure 6. Conceptual model of paleo and modern marsh profiles. The marsh platform is built on Pleistocene outwash sands, initially overlaid by high marsh peat, followed by a slow rate of transition to low marsh. During the late Holocene relative sea level rose at a rate of approximately 1.1 mm/yr, resulting in a relatively stable marsh surface dominated by high marsh plant communities. In the modern marsh, a current rate of relative sea-level rise of 3.2 mm/yr results in transgression of low marsh vegetation over the past high marsh. The high marsh is unable to keep up with the current rate of eustatic sea-level rise and has lost elevation within the tidal frame, leading to a loss in its spatial extent concurrent with replacement by low marsh. Factors leading to the resilience of the low marsh include increased biomass production and preservation in conjunction with increased mineral deposition.

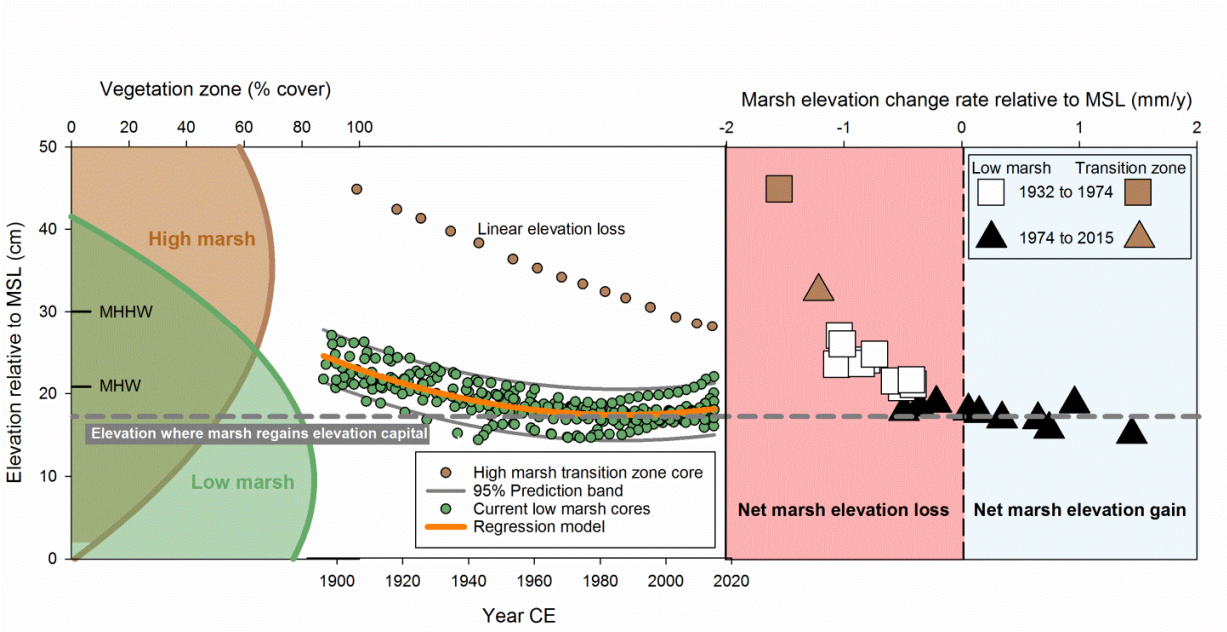

Figure 7: The position of the marsh surface relative to mean sea level (MSL) is a key driver of important biogeophysical feedbacks. On the left side of the panel, the observed elevation zones of high and low marsh vegetation are indicated relative to MSL. In the middle, the marsh surface elevation within the tidal frame over the past century is shown for current low marsh (10 cores) and the high marsh transition zone (SLPB, 1 core). The high marsh transition zone has steadily lost elevation within the tidal frame, while the present-day low marsh sites have had a more dynamic response. At right, the marsh accretion response relative to sea-level rise is shown. From 1932 to 1974, the marsh platform lost elevation within the tidal frame (red zone), while since 1974, elevation of many of the modern-day low marsh sites have stabilized. Once the marsh elevation reaches the zone where low marsh vegetation dominates (dashed gray line), the elevation change rate becomes positive (blue zone) and the marsh regains elevation within the tidal frame.

Table 1.

Lab No.	Latitude °N	Longitude °W	Depth in Core (cm)	Depth NAVD 88 (cm)	^{14}C Age (years)	2σ cal BP Median Prob. (years)	2σ cal AD Median Prob. (years)	δ^{13}C ‰	Δ^{14}C	Material Dated	RSL Point
OS-109781	41.55479	-70.5065	34	-18	100 ±25	110 ±32	1840 ±32	-11.9	-19.87	*S. patens*	SLIP
OS-109782	41.55479	-70.5065	40	-24	190 ±20	178 ±37	1772 ±37	-25	-30.6	*S. patens*	SLIP
OS-109957	41.5548	-70.5066	43	-29	180 ±20	183 ±36	1767 ±36	-16.25	-29.55	*S. patens*	SLIP
OS-109784	41.55481	-70.5067	52	-45	370 ±20	447 ±52	1503 ±52	-11.74	-52.34	*S. patens*	SLIP
OS-109780	41.55481	-70.5067	58	-51	470 ±20	516 ±20	1434 ±20	-13.27	-63.75	*D. spicata*	Limit
OS-109961	41.5548	-70.5068	68	-55	580 ±20	607 ±34	1343 ±34	-12.73	-76.83	*D. spicata*	SLIP
OS-109778	41.5548	-70.5068	78	-65	660 ±25	611 ±60	1339 ±60	-13.44	-85.8	*D. spicata*	Limit
OS-109783	41.5548	-70.5068	85	-72	620 ±20	599 ±57	1351 ±57	-11.74	-81.35	*S. patens*	SLIP
OS-109959	41.55481	-70.5068	98	-88	905 ±20	854 ±65	1096 ±65	-12.75	-113.4	*D. spicata*	SLIP
OS-109777	41.55481	-70.5068	105	-95	970 ±20	861 ±70	1089 ±70	-25.33	-120.4	*D. spicata*	SLIP
OS-109956	41.55481	-70.5068	109	-99	950 ±20	852 ±23	1098 ±23	-23.79	-118.5	*bulk*	Limit
OS-109960	41.55481	-70.5069	118	-106	1180 ±45	1109 ±76	841 ±76	-25.39	-142.9	*bulk*	Limit
OS-109774	41.55481	-70.5069	125	-113	970 ±25	860 ±73	1090 ±73	-11.81	-120.4	*D. spicata*	Limit
OS-109958	41.55485	-70.5071	31	-134	1260 ±30	1218 ±63	732 ±63	-24.04	-151.9	*bulk*	Limit
OS-109775	41.55483	-70.507	138	-126	1240 ±20	1211 ±52	739 ±52	-23.57	-149.2	*J. gerardii*	Limit
OS-109779	41.55485	-70.5071	148	-151	1500 ±20	1380 ±33	570 ±33	-25.16	-177	*D. spicata*	Limit
OS-109724	41.55483	-70.507	151	-142	1240 ±20	1211 ±52	739 ±52	-23.51	-149.5	*J. gerardii*	SLIP